ACCSCIENCE PUBLISHING

International Journal of Bioprinting

REVIEW ARTICLE

3D-printed/bioprinted systems for spatially and temporally controlled drug delivery within tumor microenvironment

Yuan Wu[1]*, Yaying Xu[1], Jukai Zhang[1], Yile Wang[1], Zhouyi Sun[2]*, and Zihao Guo[1]*

[1]College of Jiyang, Zhejiang A&F University, Zhuji, China

[2]Department of General Surgery, Center for Oncology Medicine, the Fourth Affiliated Hospital of School of Medicine, and International School of Medicine, International Institutes of Medicine, Zhejiang University, Yiwu, China

Abstract

The pronounced spatial heterogeneity and dynamic evolution of the tumor microenvironment represent key factors limiting the sustained therapeutic efficacy of anti-tumor drugs in solid tumors. Traditional drug delivery strategies often rely on spatiotemporally uniform delivery profiles, making it difficult to match the complex structural organization and continuously evolving biological states within tumor tissues. This results in uneven drug distribution, limited therapeutic windows, and the development of drug resistance. In recent years, 3D-printing and bioprinting technologies, as layer-by-layer manufacturing methods based on digital design, have provided new solutions for constructing drug delivery systems with modifiable structures, partitioned spatial organization, and programmable time-release capabilities. By precisely controlling the arrangement of materials, bioactive molecules, and cells in three-dimensional space, these systems can not only achieve fine spatiotemporal regulation of the drug delivery process but also integrate cells, extracellular matrix, and mechanical cues during delivery, thereby partially reshaping the tumor microenvironment. This paper systematically reviews the design strategies and latest advancements of 3D-printing and bioprinting delivery systems in achieving spatiotemporally controllable drug delivery within the tumor microenvironment, focusing on their advantages in spatial regulation, temporal response, and tumor microenvironment reprogramming, while analyzing the current key challenges and clinical translation prospects, aiming to provide references for the rational design of next-generation tumor delivery systems.

Keywords: 3D-printed; Bioprinted; Drug delivery; Tumor microenvironment; Clinical translation

***Corresponding authors:**
Zihao Guo
(guozihao@zafu.edu.cn)
Zhouyi Sun
(sunze1209@zju.edu.cn)
Yuan Wu
(yuanwu@zjyc.edu.cn)

Citation: Wu Y, Xu Y, Zhang J, Wang Y, Sun Z, Guo Z. 3D-printed/bioprinted systems for spatially and temporally controlled drug delivery within tumor microenvironment. *Int J Bioprint*. 2026;12(3):026170149. doi: 10.36922/IJB026170149

Received: April 22, 2026

Revised: May 25, 2026

Accepted: June 5, 2026

Published online: June 6, 2026

1. Introduction

Cancer remains one of the most challenging diseases globally, with treatment failure often attributed not to the inherent efficacy of the drugs themselves, but to their inefficient delivery and limited persistence within tumor tissues.[1,2] The tumor microenvironment (TME) of solid tumors is highly complex and heterogeneous in both spatial architecture

and temporal dynamics. This includes abnormal vascular networks, a dense and heterogeneous extracellular matrix, steep gradients of oxygen and nutrients, and a dynamic cellular composition and signaling state.[3,4] This dynamic, multi-scale microenvironment not only poses formidable physical and biological barriers but also actively drives tumor cells to undergo adaptive reprogramming to acquire drug-resistant phenotypes, thereby severely compromising the therapeutic benefits of conventional delivery strategies in clinical settings.

Despite a growing understanding of the TME, most current anti-tumor therapeutic strategies still rely on drug delivery methods that are largely uniform in both spatial and temporal dimensions. Whether administered systemically or locally, drugs typically rely on passive diffusion upon entering the tumor tissue, a process that inherently fails to align their distribution and release kinetics with the complex and dynamic characteristics of the TME.[5,6] This approach mismatches the spatial heterogeneity and temporal evolution of the TME, leading to issues including uneven drug exposure within the tumor, transient therapeutic windows, and difficulty in sustaining stable drug levels. Consequently, this not only limits therapeutic efficacy but also accelerates the onset of drug resistance.

To overcome TME-imposed drug delivery limitations, a range of advanced delivery strategies have been developed in recent years, including nanoparticle-based systemic administration, locally injected hydrogels, and intratumoral or peritumoral delivery. However, these strategies possess inherent limitations in fully addressing the spatial heterogeneity and temporal dynamics of the TME. The *in vivo* distribution of nanoparticles is primarily governed by hemodynamics, vascular permeability, and the interstitial space architecture, resulting in a highly random and heterogeneous deposition within the tumor.[7,8] Although injectable hydrogels can form local drug depots, their release behavior is predominantly dictated by material degradation or diffusion, leading to a relatively uniform release profile that is difficult to actively modulate in response to dynamic changes in the TME.[9-11] Furthermore, while local or intratumoral delivery can enhance local drug concentrations, drug diffusion within the tissue often remains poorly controlled and is influenced by tissue density and pressure gradients, resulting in unpredictability in exposure range and therapeutic outcome.[12,13] Consequently, such strategies can often only mitigate delivery challenges on a local or short-term basis and fall short of achieving sustained regulation that meets the multi-regional, multi-stage therapeutic demands of the TME.

The fundamental challenge in tumor drug delivery lies not only in material responsiveness or targeting capability, but also in achieving spatiotemporal control over drug distribution and release within tumor tissues. In this context, 3D-printing and bioprinting should be regarded not as universal substitutes for conventional delivery systems, but as complementary manufacturing strategies that are particularly valuable when therapeutic performance hinges on predefined architecture, spatial compartmentalization, region-specific drug loading, sequential release, or patient-specific construct design. Compared to nanoparticles, injectable hydrogels, and conventional local delivery approaches, these digital, layer-by-layer technologies facilitate the spatial organization of materials, bioactive molecules, and cells in three dimensions, thereby offering distinct system-level advantages for localized tumor therapy and the prevention of postoperative recurrence.[14-18] Concurrently, conventional systems may still be preferable for applications necessitating systemic administration, straightforward formulation, minimally invasive deployment, or large-scale manufacturing. This underscores that the added value of 3D- printing primarily resides in delivery scenarios where structural design and temporal programming are crucial determinants of therapeutic performance. Furthermore, bioprinting can further integrate living cells, extracellular matrix (ECM) components, and biophysical cues into delivery constructs, transforming these systems from passive carriers to active microenvironment-modulating platforms. In this review, we define 'bio-intelligent platforms' as printed delivery systems that incorporate living cells, cell-derived components, or biologically responsive modules capable of sensing, responding to, or reshaping local TME cues. This allows for the integrated modulation of tumor-immune interactions, ECM properties, and biochemical signaling, thereby extending the functional paradigm of the delivery system from a passive 'carrier' to an active 'microenvironment-modulating platform'.[19]

This paper presents a systematic review of recent advances in 3D-printing and bioprinting technologies for achieving spatiotemporally controlled drug delivery within the TME. We focus on the design principles underlying various printing strategies for constructing modulatable architectures, achieving spatial compartmentalization, and enabling temporal regulation, as well as their impact on drug delivery behavior. Additionally, we highlight the distinct capabilities of bioprinting systems in modulating key structural and functional features of the TME. Furthermore, this paper discusses the current challenges facing 3D-printed delivery systems—including biocompatibility, manufacturing complexity, and clinical translation—and provides perspectives on future directions and potential applications.

2. Characteristics of the TME relevant to drug delivery

Compared to normal tissues, the TME is characterized by profound remodeling in terms of vascular architecture, ECM composition, immune cell distribution, and metabolic status, thereby establishing multiple physical and biological barriers that collectively hinder homogeneous drug distribution and sustained therapeutic action. As shown in Figure 1, the barriers associated with the TME exhibit significant heterogeneity and are subject to dynamic evolution. A comprehensive understanding of these TME characteristics governing drug delivery is a fundamental prerequisite for the rational design of advanced delivery strategies, particularly those aimed at achieving spatiotemporal control.

2.1. Abnormal tumor vasculature

The tumor vascular system serves as the primary route for anti-tumor drugs to access tumor tissues, yet its structure and function differ significantly from those of normal blood vessels. Tumor vessels typically exhibit irregular morphology, disorganized branching, heterogeneous lumen dilation, and discontinuous endothelial junctions.[20] These architectural abnormalities lead to a certain degree of vascular hyperpermeability, but they also result in highly heterogeneous perfusion and intermittent blood flow, thereby impairing convection-dependent drug transport to deeper tumor regions.

Historically, the enhanced permeability and retention (EPR) effect has been considered a key mechanism governing the passive accumulation of nanomedicines in tumors.[21] However, a growing body of evidence indicates that the EPR effect exhibits substantial heterogeneity across tumor types, stages, and individuals, and even demonstrates marked spatial heterogeneity within a single tumor.[22,23] This functional heterogeneity of the tumor vasculature poses a significant challenge for conventional drug delivery systems—which often rely on a single administration route or homogeneous delivery strategies—to achieve stable and predictable therapeutic outcomes, frequently resulting in a heterogeneous, patchy drug distribution within the tumor and the formation of 'protected zones' that remain inadequately treated.

The regional heterogeneity in permeability and perfusion of tumor blood vessels directly dictates the initial drug accumulation and distribution patterns within the tumor tissue. This heterogeneity necessitates that delivery systems are capable of achieving region-specific drug exposure, with varying levels in perivascular and distal areas, and are designed to structurally or functionally support zonation, targeted delivery, or gradient distribution. Currently, drug delivery systems designed to target the heterogeneous tumor vasculature have reached an advanced stage of development. For instance, Kim *et al.*[24] used tumor cell-derived small extracellular vesicles (sEVs) as carriers and displayed targeting peptides specific

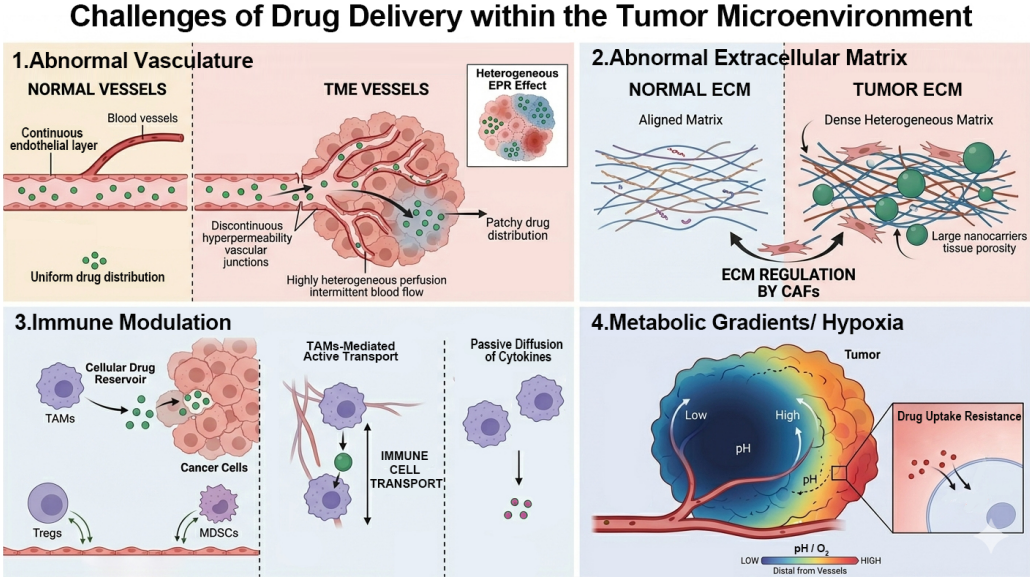

Figure 1. Schematic representation of the key biological and physical barriers within the TME that hinder effective drug delivery
Abbreviations: CAFs: Cancer-associated fibroblasts; ECM: Extracellular matrix; EPR: Enhanced permeability and retention; MDSCs: Myeloid-derived suppressor cells; TAM: Tumor-associated macrophage; TME: Tumor microenvironment; Tregs: Regulatory T cells.

to vascular endothelial growth factor receptors on their surface, thereby enabling more efficient, targeted drug delivery to peritumoral vessels and throughout the tumor tissue, which enhanced anti-tumor effects.

2.2. Dense and heterogeneous ECM

Upon crossing the vascular barrier, drugs must further diffuse through the tumor stroma to reach their target cells, a process that is significantly impeded by the ECM. Compared to normal tissues, the tumor ECM is frequently subjected to aberrant remodeling, characterized by excessive deposition of matrix components, including collagen fibers and hyaluronic acid, as well as alterations in fiber alignment and cross-linking density.[25] This ECM densification substantially reduces tissue porosity and increases diffusional resistance, thereby limiting the effective penetration of both small-molecule drugs and nano-delivery systems into the tumor.[26,27]

Moreover, the tumor ECM is spatially heterogeneous, exhibiting marked regional variations in composition, mechanical properties, and degradation status. This heterogeneity further complicates the prediction of drug diffusion kinetics within tumors, often leading to preferential drug accumulation in perivascular regions while failing to achieve uniform distribution throughout the tumor parenchyma. Notably, the ECM dynamically regulates the architecture of the tumor stroma through dynamic interactions with cancer-associated fibroblasts (CAFs) and immune cells, thereby further amplifying the spatiotemporal uncertainty inherent to the drug delivery process.[28]

2.3. Immune components of TME

The abundant immune cells infiltrating the TME not only participate in tumor progression and immune evasion but also play a critical, yet often overlooked, regulatory role in drug delivery. Immune cells such as tumor-associated macrophages (TAMs), myeloid-derived suppressor cells (MDSCs), and regulatory T cells (Tregs) typically exhibit a highly organized spatial distribution within tumor tissues, thereby forming distinct immune niches.[29-31] This heterogeneous distribution of immune niches can directly influence the intratumoral fate of drugs and nanocarriers. For instance, Miller *et al.*[32] first demonstrated that nanocarriers are extensively captured by TAMs within the TME, leading to their accumulation within TAMs and the formation of a 'cellular drug reservoir'. These TAMs then gradually release the drugs to adjacent tumor cells, thereby influencing the distribution and long-term retention of the carriers within the tumor. Furthermore, research by Lin *et al.*[33] revealed that TAMs not only capture nanocarriers but can also actively transport them through the tumor stroma toward the interior, resulting in a penetration depth that is 2- to 5-fold greater than that achieved by passive diffusion alone. These findings indicate that the distribution and retention behaviors of nanocarriers within tumors are governed not only by the EPR effect but also by active, cell-mediated transport processes.

Immune cells can indirectly modulate tumor vascular permeability and ECM architecture through the secretion of cytokines, growth factors, and matrix-remodeling enzymes, thereby influencing drug transport kinetics and therapeutic efficacy within tumors.[34] More importantly, the immunosuppressive microenvironment can attenuate the therapeutic efficacy of drugs even after successful delivery, meaning that successful delivery does not necessarily guarantee significant therapeutic outcomes. Therefore, from a drug delivery perspective, considering the immune landscape as a dynamic regulator of both transport and efficacy is critical for the development of more therapeutically integrated delivery systems.

2.4. Hypoxia and acidosis

Beyond the aforementioned physical and biological barriers, the role of chemical barriers in drug delivery must not be underestimated. Owing to aberrant vascular architecture and heterogeneous perfusion, pronounced hypoxia, acidity, and nutrient gradients are commonly observed within solid tumors.[35,36] These metabolic characteristics are spatially heterogeneous and evolve dynamically with tumor progression and treatment. Hypoxic regions, typically located deep within the tumor and distal from functional blood vessels, not only impede effective drug delivery but also induce metabolic reprogramming in tumor cells and activate drug resistance-associated signaling pathways.[4,37]

Concurrently, the acidity of the TME can influence drug stability, ionization state, and cellular uptake efficiency. For example, Ahmed *et al.*[38] reported that under acidic conditions, the cellular uptake of doxorubicin in MCF-7 and MDA-MB-231 cells was significantly reduced, leading to an increased IC_{50}—a phenomenon attributed to the drug becoming trapped in the acidic extracellular environment, which hinders its intracellular penetration. These complex and dynamic physicochemical cues pose a significant challenge for conventional delivery systems in achieving uniform and sustained therapeutic effects across different tumor regions, while simultaneously offering critical design criteria for the development of advanced delivery systems with environmental responsiveness and temporal control. Therefore, delivery systems can be engineered to exhibit temporally programmable release profiles or to trigger drug release in response to local physicochemical cues, thereby ensuring sustained and effective drug exposure

within regions characterized by unfavorable metabolic conditions and heightened drug resistance.[39,40]

In summary, the TME represents a multifaceted and dynamic barrier system that impedes drug transport, distribution, and efficacy on multiple levels. These inherent characteristics underscore the critical need for advanced drug delivery strategies capable of simultaneously addressing the physical, biological, and chemical barriers within the tumor.

3. Spatial control and temporal control strategies in 3D-printed/bioprinted systems

3D printing and bioprinting technologies enable the precise spatial arrangement of materials, drugs, and cells in three dimensions, offering enhanced control over both the spatial distribution and temporal release profiles of therapeutic agents. Figure 2 illustrates the conceptual framework utilized in this review, categorizing 3D-printed and bioprinted systems according to their increasing functional complexity, which ranges from acellular constructs to cell-laden systems and bio-intelligent platforms. Within this framework, acellular systems primarily depend on structural design and material-driven release kinetics, while cell-laden and bio-intelligent platforms integrate biological activity, feedback responsiveness, or TME modulating functions. To elucidate the relative advantages, limitations, and applicable scenarios of these approaches, Table 1 presents a strategy-oriented comparison of the principal design principles discussed in this section. Concurrently, Table 2 summarizes representative studies, detailing their release systems, passive or responsive release modes, printing technologies, materials, cell components, and key advantages.

3.1. Acellular systems

Currently, research on 3D-printed drug delivery systems has primarily focused on acellular constructs, where therapeutic functionality is heavily dependent on the synergistic optimization of material properties and structural design. This section will systematically review the design strategies employed in acellular 3D-printed platforms for engineering spatially controlled release profiles, organized around two core design dimensions: structural configuration and material selection. It will highlight how distinct geometric designs, spatially compartmentalized architectures, and functional material combinations confer upon the system predictable release kinetics and the capacity for region-specific drug distribution.

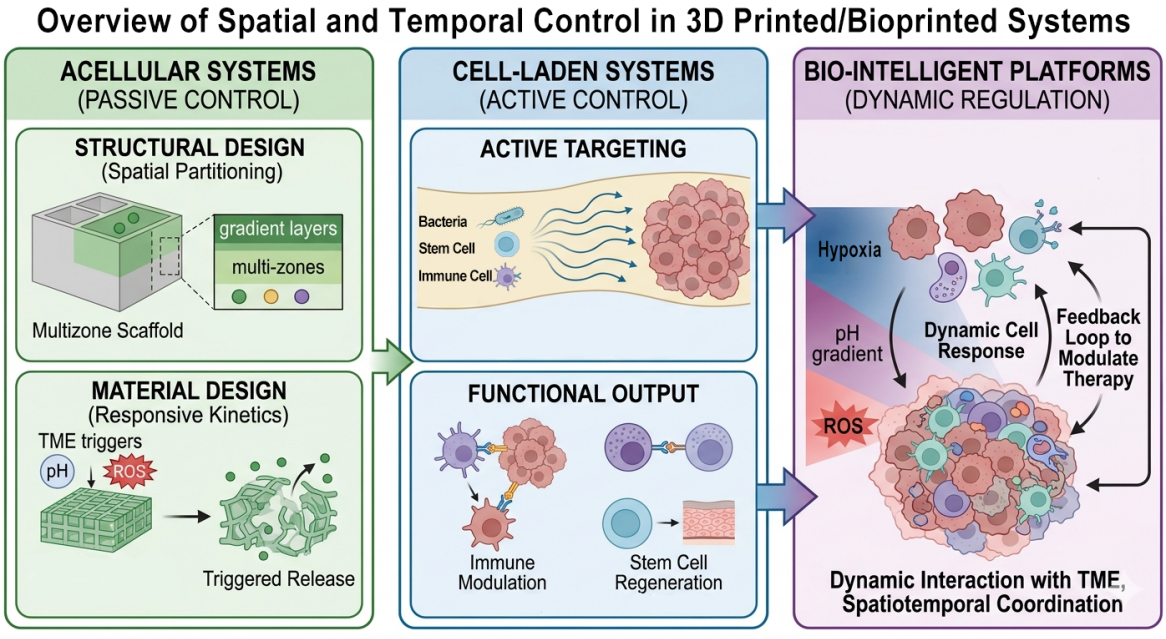

Figure 2. Progressive design strategies for 3D-printed delivery systems: From acellular scaffolds and cell-laden systems to bio-intelligent living drug factories
Abbreviations: ROS: Reactive oxygen species; TME: Tumor microenvironment.

3.1.1. Spatial partitioning and multi-region design

In 3D-printed delivery systems, the precise spatial arrangement of drugs within the 3D architecture of the printed constructs is a core strategy for achieving region-specific drug concentrations within heterogeneous tumor tissues. Leveraging digital design and layer-by-layer additive manufacturing enables the fabrication of delivery scaffolds or carriers with multiple functional zones, each tailored with distinct drug loadings, dosages, or release mechanisms, thereby achieving spatially targeted release profiles.

First, the geometric configuration of the 3D structure itself can directly dictate drug diffusion pathways and subsequent release kinetics. Without modifying the material composition, distinct release profiles can be achieved by programming the internal spatial architecture. Xu *et al.*[41] fabricated a soluble scaffold using polyvinyl alcohol (PVA) filaments and designed three distinct internal geometric configurations—cylinder, horn, and reverse horn (R-horn). By subsequently injecting a drug-loaded PVA gel at room temperature, they achieved distinct drug release profiles, including increasing, decreasing, and near-zero-order release kinetics. This study demonstrates that geometric configuration can serve as an independent regulatory variable, enabling the precise programming of drug release kinetics and establishing a theoretical foundation for spatially compartmentalized design. Similarly, numerous studies have confirmed that marked differences in release kinetics can be achieved by solely modulating 3D architectural parameters, further validating the dominant role of geometric architecture in dictating delivery performance.[42,43]

Building on this foundation, researchers further advanced the concept of "structure dictating function" to multi-compartment spatial partitioning systems. Myung *et al.*[44] developed a 3D-printed implantable device featuring multiple independent chambers that enable precise control over channel diameters, wall thicknesses, and chamber volumes, allowing for the independent programming of drug release onset times and release durations. This multi-compartment design enables the integration of multiple release schedules within the same implant, thereby overcoming the temporal coupling constraints inherent to conventional single-compartment delivery systems. More importantly, in a subsequent study, this platform was employed to simulate a clinical chemotherapy regimen combining doxorubicin and cyclophosphamide for triple-negative breast cancer, achieving highly controllable replication of drug dosage, administration frequency, and treatment cycles through its compartmentalized architecture (Figure 3A).[45] A similar spatial compartmentalization strategy has also been adopted to enhance the functionality of clinical implantable devices. Hagan *et al.*[46] employed continuous liquid interface production (CLIP) technology to fabricate biodegradable, inert polymer spacers, which were subsequently loaded with docetaxel and dexamethasone. These drug-loaded spacers are dimensionally and morphologically consistent with commercially available clinical radiotherapy spacers, enabling direct replacement of existing devices while simultaneously incorporating localized chemotherapy and anti-inflammatory functions.

The spatial compartmentalization design of 3D-printed delivery systems is often integrated with environmentally responsive release strategies. Inspired by fish morphology, Li *et al.*[47] fabricated a biomimetic microrobot comprising a magnetic scaffold (Fe_3O_4 nanoparticles embedded in poly(ethylene glycol) diacrylate, PEGDA), a drug-laden head, and a drug-laden body (gelatin methacryloyl, GelMA) (Figure 3B). The magnetic scaffold endows the system with magnetic responsiveness, enabling active targeting under an external magnetic field, while the head and body are respectively loaded with acetylsalicylic acid and doxorubicin. This design replaces the conventional multi-carrier approach with functional compartmentalization within a single structure, thereby ensuring coordinated delivery and temporal synchronization of the two drugs at the tumor site. Subsequently, the GelMA component undergoes enzymatic degradation within the TME, thereby enabling on-demand drug release. Hierarchical structures can also enable the design of spatially controlled release programs. Fang *et al.*[48] reported a 'sandwich'-structured implantable drug delivery system designed for the prevention and treatment of postoperative tumor recurrence and metastasis. The outer layer comprises a 3D-printed scaffold loaded with combretastatin A4 phosphate (CA4P), while the inner layer consists of electrospun fiber mats incorporating tirapazamine (TPZ). CA4P is preferentially released to disrupt the tumor vasculature and induce hypoxia, while the subsequently released TPZ is bioreduced in this exacerbated hypoxic environment to generate cytotoxic free radicals, thereby achieving hypoxia-dependent synergistic cytotoxicity. This sequential release is programmatically controlled through spatial isolation between the layers, establishing a therapeutic paradigm of "structure-triggered, environment-amplified, drug-synergized" action. Such compartmentalized designs are also widely employed to construct programmed therapeutic platforms that "first modulate the microenvironment, then enhance cytotoxicity," achieving precise spatiotemporal coordination of combination therapy through physical compartmentalization.[49]

In summary, spatial compartmentalization and multi-region design enable drug release to transition from being governed solely by individual material properties to being dictated by programmable, structure-mediated behavior, achieved through the precise arrangement of geometric designs, compartmentalization, hierarchical organization, and functional modularization. Such strategies offer a versatile engineering strategy to address challenges such as heterogeneous drug distribution within tumors and the temporal coordination of combination therapies, while also establishing a foundation for future integration with temporal control and microenvironment-responsive mechanisms.

3.1.2. Tailoring microstructure and porosity

Beyond macroscale geometric design, the pore size, channel orientation, and material organization within the printed scaffold also govern drug diffusion pathways within the tumor stroma. By modulating pore interconnectivity and introducing anisotropic architectures, it is possible to mitigate the diffusional resistance imposed by the dense tumor stroma, thereby enhancing drug penetration depth. This "diffusion pathway engineering" approach is emerging as a key strategy for enhancing the efficiency of local drug delivery.

Yi *et al.*[50] reported the first 3D-printed drug delivery patch designed for local inhibition of pancreatic cancer growth. The researchers employed pneumatic extrusion-based 3D-printing to fabricate a composite scaffold comprising poly (lactide-co-glycolide) (PLGA) and polycaprolactone (PCL), featuring a precisely programmable internal pore architecture and drug-loaded regions. The results demonstrated that different pore morphologies significantly influenced the release kinetics of 5-fluorouracil (5-FU), with the lattice architecture exhibiting higher drug release and a more homogeneous diffusion profile compared to the oblique and triangular designs. This study highlights that pore geometry not only influences the release rate but also directly dictates the spatial diffusion pattern of the drug within the tumor tissue.

However, for printed patches intended for intraoperative or postoperative use, optimizing pore structure alone is insufficient to address key clinical challenges; factors such as adhesion stability on irregular wound surfaces and mechanical anchoring capability are equally critical. Therefore, structural design strategies have begun to evolve from "internal diffusion regulation" to "device-tissue interface engineering." Hagan *et al.*[51] reported a custom-designed implantable chemotherapy device based on CLIP technology, aimed at preventing local recurrence after tumor resection. This system employs polyethylene glycol dimethacrylate M_n 550 (PEG_{550}-DMA) and hydroxyethylmethacrylate (HEMA) as the photo-crosslinkable resin substrate and is loaded with paclitaxel and cisplatin. The key innovation lies in the seamless integration of 3D geometric design with real-time intraoperative fabrication: an array of arrow-shaped protrusions provides mechanical anchoring to the surgical wound, while the main body is engineered to ensure sustained drug release over several weeks through modulation of crosslinking density and drug layer thickness. At a finer length scale, structural engineering has been further extended to transdermal delivery systems. Joo *et al.*[52] employed projection-based micro-stereolithography to fabricate self-locking, dissolving microneedle patches for long-term transdermal immunotherapy of melanoma. By leveraging high-resolution 3D-printing, the researchers overcame the geometric constraints of conventional fabrication methods to design a 3D self-locking architecture comprising sharp-tip piercing elements, wide-body tissue-interlocking features, and flexible, hydrophilic bases. This design significantly enhanced the piercing accuracy and attachment stability of the microneedles on irregular tumor surfaces, thereby achieving sustained anchoring over several weeks. This study demonstrates the potential of microscale 3D architectural design to overcome the challenge of long-term fixation within the dynamic skin microenvironment.

Beyond macropore and interfacial design, the microstructural gradient within scaffolds can also modulate drug release kinetics. Previous studies have shown that the architecture of highly porous 3D-printed composite scaffolds—including pore interconnectivity and size—can significantly modulate the release profiles of incorporated drugs. Furthermore, gradient pore architectures modulate diffusion pathways and mass transport efficiency within the scaffold. Such gradient structures hold promise for the precise tuning of release characteristics in drug delivery systems.[53-55]

In summary, from pore-scale modulation and channel orientation to interfacial anchoring design, the multi-level structural engineering of 3D-printed scaffolds is fundamentally reshaping the diffusion kinetics and functional stability of localized tumor delivery systems. This multiscale structural regulation, from macro to micro features, offers a novel engineering strategy to overcome the tumor stroma barrier and enhance homogeneous drug distribution within tissues.

3.1.3. Engineering controlled release and regulating release kinetics

By tailoring material composition and degradation rates, predictable release profiles can be achieved over macroscopic timescales, thereby enabling staged drug exposure. However, this pre-programmed release strategy remains fundamentally a passive control approach, as the release behavior is dictated primarily by the intrinsic degradation kinetics of the materials rather than by real-time biological cues from the TME. Given that the TME is defined by a weakly acidic pH (approximately 6.5–7.0), hypoxia, elevated reactive oxygen species (ROS) levels, and aberrant protease expression, delivery systems that rely solely on fixed degradation rates are inherently limited in their ability to achieve truly on-demand drug delivery. In this context, 3D-printed material systems that are responsive to TME signals are emerging as a central paradigm in the design of advanced delivery systems.

Leveraging the acidic TME, pH-sensitive nanocarriers have been integrated with 3D-printed scaffolds to create localized drug delivery platforms for tumor therapy. For instance, Fan *et al.*[56] developed a composite local delivery system that integrates a pH-responsive paclitaxel prodrug into a 3D-printed titanium alloy scaffold, designed for bone defect repair and recurrence prevention following osteosarcoma resection. This system exploits the acidic TME to trigger the release of the prodrug, thereby highlighting the potential of TME-responsive drug delivery strategies. Beyond incorporating pH-responsive drugs into 3D-printed scaffolds, the scaffold materials themselves can be engineered to exhibit pH-responsive behavior. Zaer *et al.*[57] reported a 3D-printed pH-responsive drug delivery system designed for breast cancer therapy. The researchers functionalized niosomes loaded with doxorubicin (Nio-DOX) and encapsulated them within a 3D-printed gelatin-sodium alginate nanocomposite scaffold, thereby constructing the Nio-DOX@GT-AL system. The pH-responsive behavior arises from pH-dependent structural changes in the gelatin-alginate matrix within the acidic TME, thereby enabling programmed release of doxorubicin. In a related approach, Kefayat *et al.*[58] utilized pH-responsive gelatin materials to construct a pH-sensitive, drug-loaded nanoparticle implant by 3D-printing a gelatin/polycaprolactone/hydroxyapatite (Gel/PCL/HA) matrix, achieving a system that integrates localized controlled release of nanoparticles with systemic delivery capability. This design concept has also been validated in other recent 3D-printed pH-responsive scaffolds—for example, through the use of tunable mesoporous silica materials that exhibit pH-dependent release behavior—further supporting the potential of acidic TME-responsive strategies.[18]

Beyond acidic TME-responsive designs, strategies designed to respond to hypoxia and redox states have also garnered increasing attention. The 'sandwich'-structured implantable composite designed by Fang *et al.*[48] is designed to prioritize the release of the drug from its outer layer following tumor resection and implantation. This released agent disrupts pre-existing tumor vasculature and inhibits neovascularization, thereby exacerbating hypoxia within the TME. Subsequently, the inner-layer TPZ is released and bioreduced to its cytotoxic form (BTZ) within this hypoxic environment, leading to synergistic suppression of tumor recurrence and metastasis. Reactive oxygen species (ROS)-responsive release represents another key mechanism in TME-responsive drug delivery. Given the marked elevation in inflammatory responses and oxidative stress following tumor resection, ROS can serve as an endogenous trigger for drug release. For instance, Wang *et al.*[59] reported a 3D-printed intelligent breast prosthesis designed for comprehensive postoperative treatment of breast cancer, which leverages this pathological feature as a trigger for on-demand drug release. The researchers incorporated a thermosensitive hydrogel loaded with the ferroptosis-inducing agent RSL3 into a 3D-printed porous scaffold. This hydrogel was synthesized by crosslinking polyvinyl alcohol (PVA) with N^1 -(4-boronobenzyl)-N^3 -(4-boronophenyl)-N,1N^1,N^3,N^3 -tetramethylpropane-1,3-diaminium (TSPBA), resulting in a ROS-responsive hydrogel network. Upon exceeding a critical local ROS threshold, the ROS-labile bonds cleave, leading to network dissociation or swelling, thereby triggering the programmed release of the antitumor drug for precise targeting at sites of recurrence (Figure 3C). Similar strategies that exploit elevated tumor ROS levels for triggered release have also been proposed and validated in other delivery systems, providing a strong rationale for the design of ROS-responsive 3D-printed systems.[60,61]

Specific enzymes overexpressed in the TME, such as matrix metalloproteinases (MMPs), along with an abnormally elevated redox potential, particularly glutathione (GSH), provide endogenous triggers for the design of smart, stimuli-responsive delivery systems. However, the integration of these mechanisms into macroscopic 3D-printed drug delivery devices remains in its infancy, with existing research largely confined to the nanoscale. This limitation arises because GSH-responsive systems typically rely on cleavable covalent bonds, such as disulfide linkages, which poses significant challenges for achieving efficient and controllable responsiveness in macroscopic 3D-printed scaffolds, particularly with regard to structural design and the preservation of mechanical

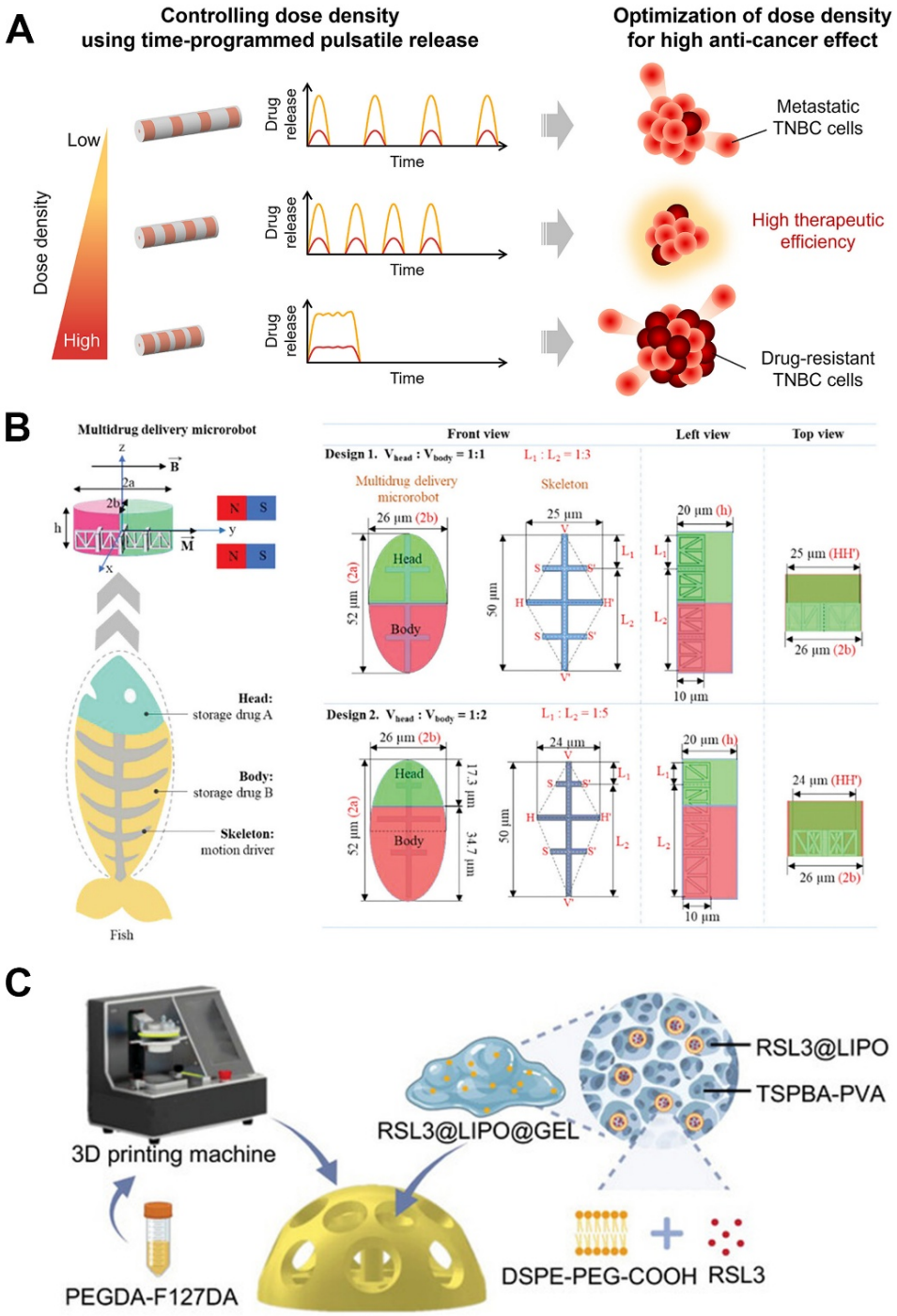

Figure 3. Engineered platforms for programmable, biomimetic, and patient-tailored drug delivery. (A) Schematic of dose density optimization using 3D-printed compartmentalized devices.[45] Reprinted with permission from Shenyang Pharmaceutical University. Copyright © 2024 Elsevier B.V. on behalf of Shenyang Pharmaceutical University. (B) Design and structural characterization of a fish-inspired biomimetic microrobot for multidrug delivery.[47] Reprinted with permission from John Wiley and Sons. Copyright © 2023 Wiley. (C) Schematic of the preparation and smart drug-release mechanism of the custom-made breast prosthesis.[59] Reprinted with permission from John Wiley and Sons. Copyright © 2024 Wiley.

integrity. Although the GSH-responsive mechanisms in 3D-printed tumor delivery systems remain underexplored, non-printed redox-responsive nanocarriers offer valuable design references. For instance, disulfide-containing hollow mesoporous silica nanoparticles can undergo GSH-triggered degradation, facilitating doxorubicin release under reductive conditions.[62] Additionally, disulfide-linked polyprodrug nanomedicines have been utilized to enable the intracellular co-release of synergistic chemotherapeutics.[63] These findings suggest that future 3D-printed systems may incorporate GSH responsiveness through two complementary approaches: embedding redox-responsive nanocarriers within mechanically stable printed scaffolds or developing dual-crosslinked bioinks. In this latter approach, a stable primary network preserves print fidelity, while secondary disulfide or diselenide-containing crosslinks regulate local degradation and drug release.

These microenvironment-responsive release strategies mark a paradigm shift from traditional "passive time-controlled" to "lesion-responsive" drug delivery by leveraging the intrinsic physicochemical characteristics of the tumor lesion as direct triggering mechanisms. This internally triggered logic not only enhances the spatiotemporal precision of localized drug release but also offers a systematic engineering framework for the design of more precise and on-demand 3D-printed drug delivery platforms.

3.2. Cell-laden systems

While acellular systems are primarily governed by material architecture and pre-programmed release kinetics, cell-laden 3D/bioprinting systems propel the functional capabilities of drug delivery platforms into a new realm through the direct integration of living cells into 3D-printed constructs. In contrast to conventional acellular scaffolds, these bioprinting systems can spatially position different cell types—such as tumor cells, immune cells, or functional cells—at predefined locations with high precision, enabling them to dynamically modulate drug delivery kinetics and TME responses through their inherent biological activity. The secretory activity, chemotactic behavior, and feedback responses of these cells offer distinct advantages for the construction of intelligent drug delivery systems capable of adaptive and functional outputs.

The incorporation of distinct live cell types can fulfill diverse functional roles and substantially enhance the therapeutic efficacy and targeting specificity of the delivery system. For instance, Kang *et al.*[64] immobilized the piezoelectric nanomaterial $BaTiO_3$ onto the surface of *Enterobacter aerogenes* (EA) to fabricate an EA@BTO biohybrid, which was subsequently encapsulated within enteric microcapsules via photopolymerization-based 3D-printing. This design represents a sophisticated integration of living cells with macroscopic printed structures within the realm of 3D-printed drug delivery. Upon reaching the alkaline environment of the intestine, the microcapsules dissolve, and the liberated EA@BTO actively targets tumor tissues and penetrates the mucus barrier by leveraging the inherent anaerobic chemotaxis of the bacteria.

Beyond bacterial-based systems, the integration of TME-resident cell types into bioprinting systems has also advanced applications in immune delivery and vaccine development. Yang *et al.*[65] reported a microneedle system for intradermal delivery of cell-based cancer vaccines. The system uses cryogenic molding to fabricate microneedle arrays loaded with tumor cell lysates or whole cells, which release active components after mechanical insertion. The controlled freezing process and resulting ice crystal morphology preserve the integrity of cell membranes within the carrier and maintain antigen activity, thereby avoiding the damage to active components typically caused by high-temperature curing in conventional solid microneedle fabrication, and enhancing both immunogenicity and delivery efficiency (Figure 4). Tumor cell-loaded systems can function as *in situ* vaccines to modulate anti-tumor immunity, whereas other approaches directly incorporate immune cells to regulate the tumor immune microenvironment. For example, Kim *et al.*[66] employed 3D-printing to encapsulate natural killer (NK) cells within porous hydrogels, enabling direct implantation at the tumor site for localized tumor killing.

Stem cells can also fulfill a functional role through their stemness properties within 3D-printed delivery systems. For instance, Xia *et al.*[67] reported a biphasic hydrogel scaffold with a core/shell fiber architecture, in which one fiber compartment is loaded with chemotherapeutic agents and incorporates photothermally responsive nanomaterials, while the other compartment encapsulates stem cells. Upon near-infrared (NIR) irradiation, this system can enable combined photothermal–chemotherapy and promote soft tissue regeneration, offering an integrated strategy for postoperative local tumor therapy and tissue regeneration. Bioprinting has been extensively utilized to develop *in vitro* tumor models characterized by specific cellular compositions, ECM-like matrices, and spatial organization. Compared to conventional two-dimensional cultures, these models more accurately replicate essential features of the TME, including 3D cell–cell and cell–matrix interactions, diffusion barriers, and heterogeneous drug responses. Consequently, they provide valuable platforms

for assessing drug penetration, release behavior, and the therapeutic efficacy of 3D printed delivery systems.[68] However, it is important to note that these systems primarily function as experimental evaluation models rather than as therapeutic delivery platforms. Thus, while their significance in the assessment of delivery systems is recognized, this review will concentrate on 3D-printed and bioprinted systems specifically engineered for direct therapeutic delivery, controlled drug release, or treatment-oriented modulation of the TME.

Nevertheless, the therapeutic application of living cells within 3D-bioprinted delivery systems presents challenges that are fundamentally distinct from those associated with acellular constructs. The viability and phenotype of cells may be compromised due to printing-related stresses, including shear forces, crosslinking conditions, and exposure to photo- or thermal stimuli.[69,70] Furthermore, allogeneic or engineered cells may provoke immune rejection, while autologous cell-based systems encounter limitations regarding scalability, reproducibility, and manufacturing standardization.[71] Another unresolved issue is whether printed cells can sustain stable functions post-implantation, as the hypoxic, acidic, nutrient-deprived, and immunosuppressive TME may hinder cell survival or induce phenotypic drift.[69] Therefore, future cell-laden platforms should be assessed not only for printing fidelity and short-term therapeutic efficacy but also for cell survival, immune compatibility, functional persistence, and *in vivo* controllability.

Fueled by advances in bioink development, bioprinting platforms, and cell engineering, cell-laden drug delivery systems are evolving from static structural constructs toward dynamic, feedback-driven systems. This concept has already been demonstrated in nano-delivery systems, where neutrophils, leveraging their inherent chemotaxis, can actively respond to local inflammation and TME signals for targeted delivery.[72] Although this approach has yet to be realized in 3D-printed delivery systems, it offers novel design paradigms and a biological rationale for the development of next-generation precision tumor delivery systems capable of synergistic therapy, immune modulation, and dynamic TME interaction.

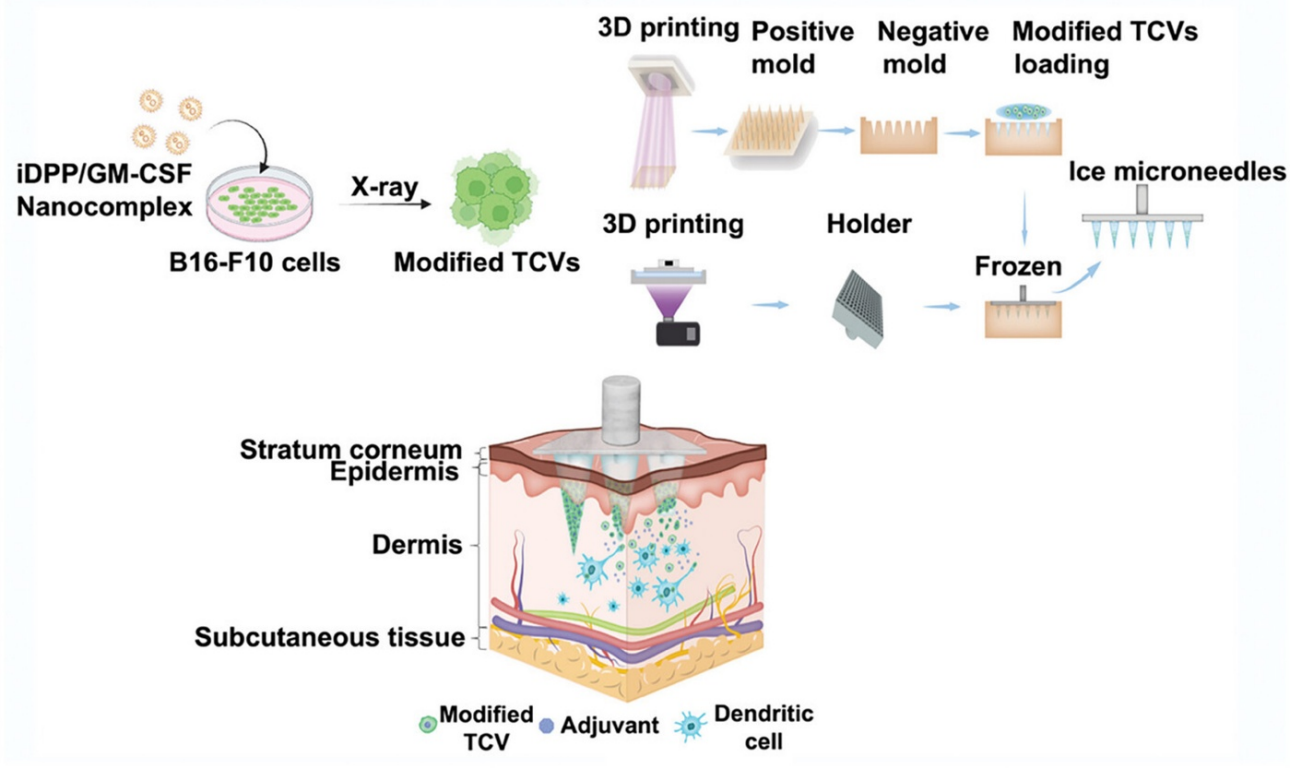

Figure 4. Cell-laden microneedle platform for localized cancer immunotherapy. The illustration shows an ice microneedle (MN) system for intradermal delivery of modified whole tumor cell vaccines (TCVs)[65]. Reprinted with permission from John Wiley and Sons. Copyright © 2024 Wiley.

Table 1. Comparative overview of major design strategies in 3D-printed and bioprinted tumor drug delivery systems

Design strategy	Primary design variable	Advantages	Key limitation	Best-fit scenarios	Ref.
Spatial compartmentalization of drugs or functional modules	Spatial placement of drugs, layers, chambers, or functional regions	Decouples different drugs or release phases, enabling regional loading, combination therapy, and sequential treatment	Requires accurate fabrication and stable compartment interfaces; limited adaptability after implantation	Localized combination therapy; postoperative recurrence prevention	44,48
Diffusion-pathway and interface engineering	Pore size, pore interconnectivity, channel orientation, scaffold geometry, and tissue-contacting interfaces	Regulates local diffusion paths, tissue retention, and scaffold–tissue interaction without necessarily changing drug chemistry	Drug transport remains influenced by local tissue density, pressure, degradation, and wound-bed geometry	Implantable patches; resection-site scaffolds; dense-stroma tumors; systems requiring prolonged local retention	50,52
Stimuli-responsive release	Endogenous or external triggers, such as pH, ROS, enzymes, hypoxia, magnetic fields, or ultrasound	Links drug release to pathological cues or external actuation, enabling more selective or on-demand therapy	Trigger intensity, penetration, and spatial distribution may be heterogeneous in vivo	TME-responsive therapy; recurrence-prone lesions; externally controllable local treatment	56,59
Cell-laden and bio-intelligent delivery	Living cells, cell-derived components, ECM cues, or biologically responsive modules	Adds biological functions such as sensing, secretion, migration, immune modulation, and TME remodeling	Cell viability, immune compatibility, functional persistence, biosafety, and manufacturing reproducibility remain major barriers	Immunomodulation; cell-based therapy; combined tumor therapy and tissue regeneration	64,66

Abbreviations: ECM: Extracellular matrix; ROS: Reactive oxygen species; TME: Tumor microenvironment.

Table 2. Summary of 3D-printed and bioprinted systems for controlled drug delivery and tissue engineering in cancer therapy

Release systems	Controlled release	3D-printing technology	3D-printing materials	Cell components	Advantages and significance	Ref.
Acellular systems	Geometric configuration programming	FDM 3D-printing	PVA filament	-	The geometric configuration can be used as an independent variable to program the release behavior.	41
Acellular systems	Multi-region and geometric configuration programming	Extrusion-based 3D-printing	Gelatin, starch, and SA	-	Bionic design and modular adjustability	42
Acellular systems	Geometric configuration programming	FDM 3D-printing	Beeswax, fenofibrate	-	Without altering the basic formula, diverse release behaviors can be achieved.	43
Acellular systems	Multi-layer structure design	Pneumatic extrusion 3D-printing; DIW 3D-printing	PCL, Pluronic F127 hydrogel	-	Supporting the sequential programming of combined therapy, its efficacy was verified to be superior to that of traditional administration in the xenograft model of triple-negative breast cancer.	44

(*Cont'd...*)

Table 2. (*Continued*)

Release systems	Controlled release	3D-printing technology	3D-printing materials	Cell components	Advantages and significance	Ref.
Acellular systems	Multi-layer structure design	Pneumatic extrusion 3D-printing; DIW 3D-printing	PCL, Pluronic F127 hydrogel	-	For the first time, local high-dose chemotherapy has been successfully applied to TNBC, achieving better therapeutic effects than intratumoral injection and with lower side effects.	[45]
Acellular systems	Unique surface design	CLIP 3D-printing	HEMA, PEG550-DMA, LTPO, BLS	-	This drug-loading spacer is consistent in size and shape with the commercially available clinical radiotherapy spacers, and can be directly substituted for the existing products.	[46]
Acellular systems	Multi-region design; magnetic response; enzyme response	Two-photon polymerization 3D-printing	GelMA, LAP, PEG	-	The external magnetic field drives the micro-robot to actively target the tumor site. The head and the body are respectively loaded with different drugs. In the TME, they are degraded by enzymes to achieve on-demand release.	[47]
Acellular systems	Multi-layer structure design; oxygen deprivation response	Pneumatic extrusion 3D-printing; DIW 3D-printing; electrospinning	Soy protein isolate, PVA, SA, poly PLGA	-	Through the design of the interlayer structure, the outer layer CA4P is the first to release and damage the blood vessels, inducing hypoxia. Subsequently, the inner layer TPZ is activated under hypoxic conditions, achieving sequential and coordinated killing.	[48]
Acellular systems	Microstructural design	Pneumatic hot-melt extrusion 3D-printing	PLGA, PCL	-	Different pore morphologies significantly affect the release behavior of 5-FU.	[50]
Acellular systems	Microstructural design	CLIP 3D-printing	HEMA, PEG550-DMA, LTPO, BLS	-	Couple the 3D geometric configuration with in situ manufacturing during the operation, achieving mechanical anchoring of the surgical wound and continuous drug release for several weeks.	[51]
Acellular systems	Microstructural design	DLP chip-based projection micro-stereolithography 3D-printing	High-temperature light-curable resin, PDMS, sodium hyaluronate	-	Design a 3D self-locking configuration consisting of a sharp puncturing end, a wide-body tissue interlocking structure, and a flexible hydrophilic base, to solve the problem of long-term fixation in a dynamic skin environment.	[52]
Acellular Systems	pH response	Electron Beam Melting 3D-printing	Titanium alloy	-	This system utilizes tumor acidic signals to trigger the release of drug-loaded prodrugs, and is used for bone defect repair and recurrence prevention after osteosarcoma surgery.	[56]

(*Cont'd...*)

Table 2. (*Continued*)

Release systems	Controlled release	3D-printing technology	3D-printing materials	Cell components	Advantages and significance	Ref.
Acellular systems	pH response	Extrusion-based 3D-printing	Gelatin, alginate	-	The gelatin/sodium alginate matrix undergoes structural changes in the acidic microenvironment of tumors, thereby enabling the programmed release of doxorubicin.	[57]
Acellular systems	pH response	Extrusion-based 3D-printing	PCL, hydroxyapatite, gelatin type B, CS	-	After implanting the 3D-printed scaffold into the abdominal cavity, it can significantly enhance the inhibition of primary tumor growth and reduce liver and peritoneal metastasis.	[58]
Acellular systems	ROS response	Extrusion-based 3D-printing	PVA, TSPBA	-	When the tumor recurs, the local ROS concentration exceeds the limit, thereby triggering the programmed release of the drug, achieving precise killing of the recurrent lesion.	[59]
Cell-laden systems	Core-shell structure design; ultrasonic response	Light-curing 3D-printing	GelMA, LAP	Enterobacter aerogenes	The microcapsules dissolve in the alkaline environment of the intestinal tract, and the released EA@BTO utilizes the inherent anaerobic chemotaxis of bacteria to actively target tumor tissues and penetrate the mucus barrier.	[64]
Cell-laden systems	Microstructural design	Static optical projection lithography 3D-printing;DLP based 3D-printing	Cryogenic medium, photosensitive resin, silica gel	Tumor cell vaccines	ntradermal delivery of live tumor cell vaccines using ice microneedles maintains the cell's viability. It also recruits dendritic cells through intradermal administration and activates the immune response.	[65]
Cell-Laden Systems	Multi-layer structure design	Extrusion-based 3D-printing	SA, gelatin	NK cells	Encapsulate NK cells in micro/mesoporous hydrogel to construct a local delivery platform suitable for cell survival and function.	[66]
Cell-laden systems	Multi-region design; near-infrared response	Extrusion-based 3D-printing	SA, gelatin	Stem cells	Realize the integration of local tumor treatment and tissue repair in the same support structure. The design of separate compartments for stem cells and drugs avoids thermal and drug damage.	[67]

Abbreviations: 3D: Three dimensional; BLS: 2 Tert butyl 6 (5 chloro 2H benzotriazol 2 yl) 4 methylphenol; CA4P: Combretastatin A 4 phosphate; CLIP: Continuous liquid interface production; CS: Chitosan; DLP: Digital light processing 3D printing; EA@BTO: Enterobacter aerogenes loaded with barium titanate; FDM: Fused deposition modelling; GelMA: Gelatin methacryloyl; HA: Sodium hyaluronate/hydroxyapatite (context-dependent); HEMA: Hydroxyethylmethacrylate; LAP: Lithium phenyl 2,4,6 trimethyl benzoyl phosphinate; LTPO: Ethyl (2,4,6 trimethylbenzoyl) phenylphosphinate; NK cells: Natural killer cells; PCL: Poly(ε caprolactone); PDMS: Polydimethylsiloxane; PEG: Polyethylene glycol; PEG550 DMA: Polyethylene glycol dimethacrylate Mn 550; PLGA: Poly(lactic co glycolic acid); PVA: Poly(vinyl alcohol); ROS: Reactive oxygen species; SA: Sodium alginate; SPI: Soy protein isolate; TME: Tumor microenvironment; TPZ: Tirapazamine.

4. Engineering the TME by 3D-printed delivery systems

3D printing technology, owing to its highly versatile design capabilities in geometric configurations, material functions, and drug delivery behaviors, enables drug carriers to not only function as passive delivery platforms but also to actively interact with key TME components, including immune cells, vascular and biochemical gradients. This section discusses the modulation of immune, vascular, and metabolic conditions within the TME by 3D-printed and bioprinted systems (Table 3).

4.1. Immune microenvironment

3D printing technology has enabled the development of various delivery systems designed to target specific

immune cell populations through the integration of immunomodulatory agents and functional materials into complex 3D architectures. Additionally, 3D-printed biocompatible porous scaffolds can be engineered to form 'artificial tertiary lymphoid structures' (aTLS) around tumors, functioning as artificial lymphoid organs that promote the recruitment and infiltration of immune cells[73]. These strategies can be broadly categorized into three main types based on their primary cellular targets: those targeting macrophages, T cells, and antigen-presenting cells.

4.1.1. Macrophage regulation

Macrophages serve as a central regulatory hub within the tumor immune microenvironment (TIME), with their polarization state—ranging from the pro-inflammatory (M1) to the anti-inflammatory (M2) phenotype—directly impacting tumor progression and prognosis. As key mediators of both pro-inflammatory, anti-tumor responses and anti-inflammatory, tissue-repair processes, the modulation of macrophages exhibits a distinctly "biphasic" nature. This biphasic requirement is particularly evident in the context of bone tumor therapy, necessitating, on one hand, the suppression of M2 polarization to alleviate immunosuppression and eliminate residual tumor cells, while on the other hand, requiring the induction of M2 polarization to promote tissue repair and bone regeneration. The architectural flexibility and functional integration afforded by 3D-printing technology provide a promising platform for achieving these seemingly contradictory immunomodulatory goals in a stage-dependent manner.

Li *et al.*[74] designed a 3D-printed calcium phosphate scaffold coated with a crosslinked hydrogel layer and loaded with a CSF-1R inhibitor, an inhibitor of the colony-stimulating factor-1 receptor (CSF-1R) on macrophages. This system enables a "dual-stage" immunomodulatory strategy for bone tumor therapy: In the first stage, sustained local release of the CSF-1R inhibitor suppresses the polarization of tumor-associated macrophages toward the immunosuppressive M2 phenotype, thereby reprogramming the immunosuppressive TIME and reducing the risk of postoperative tumor recurrence. In the second stage, following complete inhibitor release, the exposed bone-regenerative scaffold promotes tissue repair. This approach effectively transforms a 3D-printed bone scaffold from a passive mechanical support into an active immunomodulatory platform through the synergistic modulation of macrophage phenotypes via material functionalization and controlled drug release. In a subsequent study, Li *et al.*[75] employed boron–nitrogen coordination bonds to immobilize mesoporous silica nanoparticles loaded with the CSF-1R inhibitor onto the scaffold and stably conjugated anti-SIRPα antibodies to the scaffold surface, thereby achieving dual blockade of the key immunosuppressive signaling pathways—MCSF/CSF-1R and CD47/SIRPα. The CD47/SIRPα axis functions as a critical "don't eat me" signal that inhibits macrophage phagocytosis and plays a key role in tumor immune evasion[76]. This dual-blockade strategy preserves macrophage phagocytic activity while simultaneously suppressing their polarization toward the immunosuppressive M2 phenotype, thereby enhancing macrophage-mediated clearance of residual tumor cells and reducing postoperative recurrence.

Macrophage modulation extends beyond the induction of pro-inflammatory immune activation to also encompass the promotion of anti-inflammatory, tissue-repairing M2 polarization during bone regeneration following tumor resection[77,78]. Dutta *et al.*[79] reported a 3D-bioprinted, nanoengineered hydrogel scaffold fabricated by incorporating polyphenol-derived carbon quantum dots (CQDs) into a gelatin methacryloyl (GelMA) matrix. In this system, CQDs not only confer near-infrared (NIR) responsiveness for triggered anti-tumor drug release but also directly promote M2 polarization through immunomodulatory interactions, thereby promoting the osteogenic differentiation of human bone marrow mesenchymal stem cells (hBMSCs).

4.1.2. NK/T cells regulation

The exhausted phenotype of natural killer (NK) and T cells, along with the infiltration of regulatory T cells (Tregs), represent key mechanisms of tumor immune evasion. Immunomodulatory strategies targeting specific T cell subsets have yielded significant advances in both transdermal immunotherapy and localized implantable chemotherapy systems. Ranging from "relieving inhibition" to "promoting activation," diverse 3D-printed delivery platforms are now achieving multi-dimensional and precise regulation of T cell functionality.

Reversing T cell exhaustion through the alleviation of immunosuppression represents a fundamental prerequisite for restoring effective anti-tumor immunity. The self-locking, dissolvable microneedle platform designed by Joo *et al.*[52] employs 3D-printing for the co-delivery of immune checkpoint inhibitors (αPD-L1 antibody) and transforming growth factor beta (TGF-β) pathway inhibitors (SD-208), enabling sustained local release at melanoma lesion sites, thereby reshaping the functional status of T cells within the TIME. In contrast to conventional intratumoral injections, the drug-loaded patches significantly enhanced T cell infiltration and activation, notably increasing the number of $CD8^+$ cytotoxic T cells by approximately 14-fold

relative to the PBS control group. This strategy alleviates immunosuppression within the TME by concurrently suppressing immunosuppressive factors and relieving negative regulation via the TGF-β/PD-L1 signaling axis, thereby removing key suppressive signals that hinder subsequent T cell effector function. Similarly, Badiee *et al.*[80] developed a nanomedicine formulation of the GSK3 inhibitor SB415286 using a 3D-printed microfluidic chip, which was shown to effectively inhibit PD-1 expression in CAR-T cells, enhance their survival and proliferation, and increase the proportion of memory T cells, offering a novel strategy for modulating T cell function using small molecule inhibitors.

The activation of innate immunity via direct stimulation, followed by the cascading amplification of T cell responses, represents an advanced immunotherapeutic paradigm that builds upon the concept of "release of inhibition." Wang *et al.*[81] reported an implantable, coaxial 3D-printed immunomodulatory scaffold featuring a design where the STING agonist SR-717 is integrated into the outer layer and the AKT inhibitor MK-2206 is loaded into the core, thereby achieving sequential drug release. SR-717 first activates the cGAS-STING pathway, priming cytotoxic T cell responses against tumor cells, while the subsequently released MK-2206 enhances STING downstream signaling through inhibition of AKT phosphorylation. This amplified immune response significantly promotes dendritic cell (DC) maturation and M1 macrophage polarization, which in turn further potentiates T cell-mediated cytotoxicity against tumor cells. This study demonstrates the feasibility of achieving "innate-adaptive immune cascade activation" using 3D-printed scaffolds. Additionally, the injectable amino acid-based hydrogel scaffold developed by Yin *et al.*[82] functions as a delivery vehicle for the TLR7 agonist R837, forming a drug reservoir upon subcutaneous injection that enables sustained R837 release and significantly enhances $CD4^+$ and $CD8^+$ T cell responses. More broadly, a recent review by Debnath *et al.*[19] systematically summarized the critical role of 3D-bioprinting in modulating and activating key immune cells, including T cells, dendritic cells, and macrophages, laying a theoretical foundation for future innovations in immunotherapeutic strategies.

Triggering immunogenic cell death (ICD) while concomitantly remodeling the T cell-inflamed microenvironment provides an expanded source of tumor antigens to potentiate T cell activation. For instance, the RSL3@LIPO@GEL nanogel scaffold developed by Wang *et al.*[59] is designed to induce ferroptosis in tumor cells and systematically evaluates the immunomodulatory effects of this 3D-printed gel scaffold on the TIME. In the experimental group, not only was the M1/M2 macrophage ratio significantly increased, but the numbers of $CD4^+$ helper T cells and $CD8^+$ cytotoxic T cells were also markedly elevated. This observation suggests that ferroptosis-induced ICD releases tumor-associated antigens (TAAs) and damage-associated molecular patterns (DAMPs), providing ample "ammunition" for T cell priming, thereby converting the initially "cold" TME into a "hot," immunoactive state. Integrating innate immune activation with ICD induction, Li *et al.*[83] reported a layered, dual-drug reservoir, in which the STING agonist MSA-2 is loaded onto the outer layer of a 3D-printed scaffold and the ICD inducer doxorubicin (DOX) is incorporated into the electrospun inner layer, thereby achieving a programmed sequential release profile, with MSA-2 released first followed by DOX. MSA-2 not only activates the STING-IFNβ pathway but also induces endoplasmic reticulum (ER) stress-mediated immunogenic apoptosis, thereby enhancing DAMP release; while the subsequent release of DOX further amplifies STING pathway activation, thereby initiating a sustained cascade immune response that effectively suppresses postoperative tumor recurrence and metastasis (Figure 5).

4.1.3. Antigen-presenting cells regulation

Dendritic cells and other antigen-presenting cells represent the critical initiation point for adaptive immunity. Precision delivery strategies designed to target these cells have emerged as a uniquely valuable approach in cancer vaccine development.

The *in situ* recruitment and activation of dendritic cells (DCs) to elicit systemic anti-tumor immunity represents a core strategy in cancer vaccine design. Kota *et al.*[84] reported an implantable 3D-printed cancer vaccine platform, termed "NanoLymph," which features a unique dual-reservoir architecture enabling the sustained co-delivery of both immune adjuvants and tumor antigens. This platform recruits DCs to the subcutaneous site through the continuous release of granulocyte-macrophage colony-stimulating factor (GM-CSF) and CpG oligodeoxynucleotides, where they are exposed to tumor-associated antigens derived from whole-cell tumor lysates. Xie *et al.*[85] developed an injectable 3D macroporous scaffold vaccine that achieves sustained release through tunable hydrophobic interactions between a polysaccharide backbone and the TLR2 agonist acGM. This design enables sustained activation of TLR2 signaling in *in situ*-recruited DCs following subcutaneous injection, inducing intracellular ROS generation with optimized kinetics, thereby significantly enhancing antigen cross-presentation.

The direct encapsulation of functional DCs within 3D scaffolds to potentiate adoptive cell therapy represents an

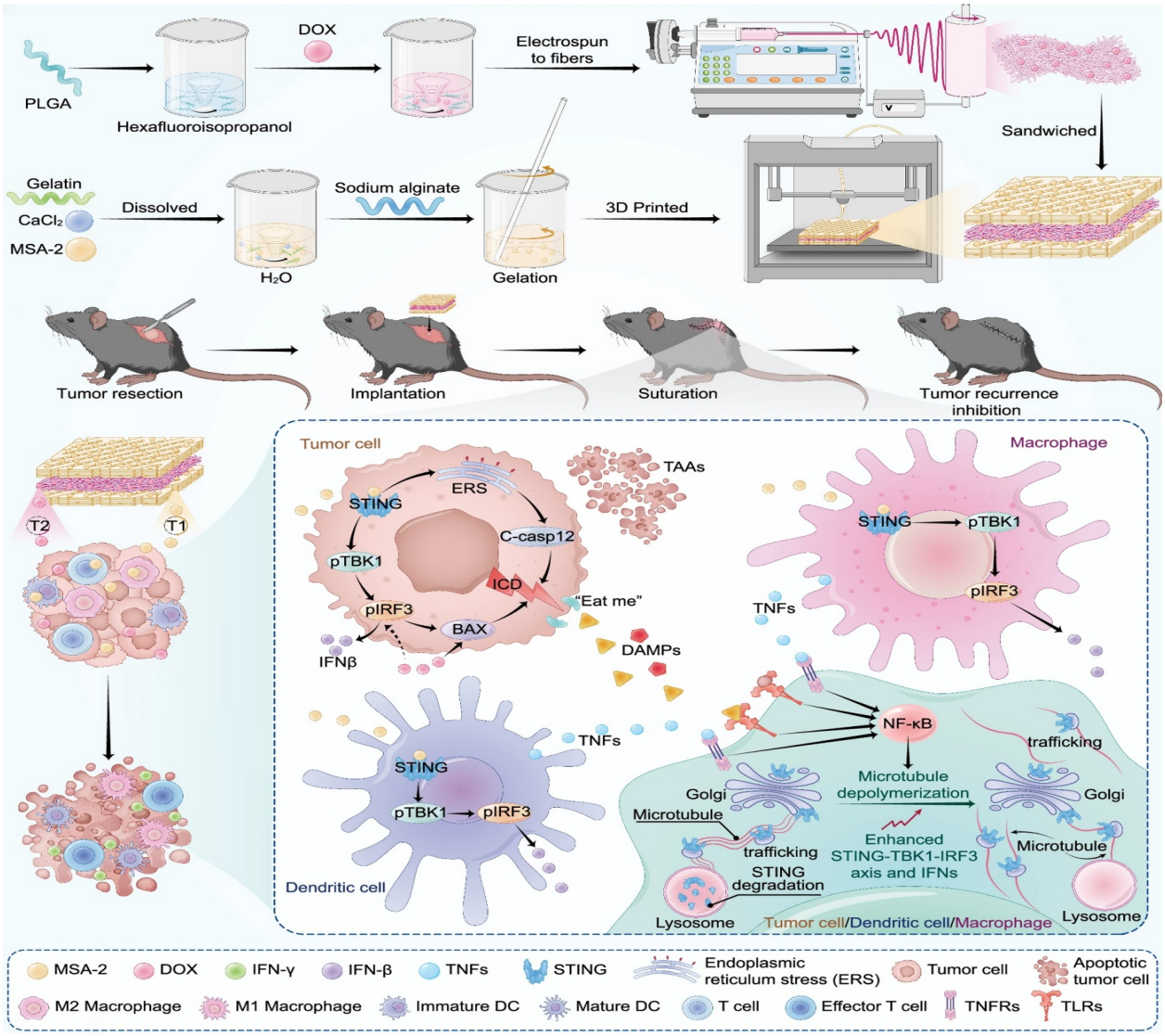

Figure 5. Layered 3D-printed scaffold for sequential immunomodulation and immunogenic chemotherapy. Fabrication and therapeutic mechanism of a 3D-printed "sandwich" drug depot for postoperative immunotherapy. Reprinted with permission from Li *et al.*[83] Copyright © 2025 Springer Nature.

alternative technological paradigm. Xu *et al.*[86] reported a 3D-printed dendritic cell vaccine in which DCs are co-encapsulated with tumor cell-derived vesicles overexpressing programmed death protein 1 (PD1-CVs) within a methacrylated gelatin (GelMA) bioink. The incorporated PD1-CVs not only stimulate DC maturation but also concurrently block PD-L1 expression on the surface of both mature DCs and tumor cells, thereby synergistically enhancing DC-mediated anti-tumor immunity. The *in situ* generation of DC vaccines at surgical sites offers an innovative strategy to circumvent the complexities of conventional DC vaccine preparation. Chen *et al.*[87] recently reported a 3D-printed scaffold-based DC vaccine designed for *in situ* generation, fabricated by simply 3D-printing a composite of GelMA, bone marrow-derived mononuclear cells (BM-MNCs), tumor lysates, and stimulatory factors. Within this system, the stimulatory factors effectively drive the *in situ* differentiation of BM-MNCs into DCs, while the incorporated tumor lysates promote the maturation of these differentiated DCs and enhance their migration to lymph nodes. This strategy entirely bypasses the complex and labor-intensive steps of *in vitro* cell culture and represents a next-generation approach for the development of simple, safe, and effective DC vaccines.

4.2. Vasculature

The vascular system within the TME represents a key physical barrier that critically regulates tumor progression and therapeutic outcomes. 3D printing technology, with its inherent capability for multi-material integration and spatial architectural programming, offers a useful strategy for the precise spatiotemporal regulation of tumor angiogenesis.

Targeting pathological angiogenesis to disrupt the tumor nutrient supply represents a key strategy for inhibiting postoperative tumor recurrence. Fang *et al.*[88] reported a layered, implantable drug delivery system in which the vascular disrupting agent combretastatin A4 (CA4) is loaded onto a 3D-printed outer scaffold and combined with electrospun inner fibers incorporating doxorubicin (DOX). The preferential release of CA4 induces vascular deformation and occlusion by disrupting endothelial cell microtubules, thereby disrupting the nutrient supply, while the subsequent release of DOX further eradicates residual tumor cells in the periphery. The indirect anti-angiogenic effects of chemotherapeutic agents add another mechanistic dimension to vascular regulation strategies. In a biomimetic multi-drug delivery microrobot system developed by Li *et al.*,[47] the co-loaded microrobots exhibited the most potent anti-tumor effect, which was accompanied by complete inhibition of angiogenesis. This study highlights the indirect regulatory effects of chemotherapeutic agents on the tumor vasculature, beyond their well-established direct cytotoxic effects on tumor cells.

Abbadessa *et al.*[89] targeted the root of angiogenesis by integrating PLGA microspheres loaded with the anti-VEGF antibody bevacizumab into a 3D-printed collagen scaffold. This system enabled sustained and programmable release of bevacizumab while preserving the scaffold's printability and structural integrity. *In vitro* studies demonstrated significant inhibition of angiogenesis in human umbilical vein endothelial cells (HUVECs), thereby establishing an implantable, functional platform for targeted anti-angiogenic therapy.

4.3. Biochemical cues

Dysregulated biochemical cues in the TME, including hypoxia, elevated ROS levels, and acidic metabolite accumulation, not only constitute key drivers of tumor malignancy but also represent a major bottleneck that impedes postoperative tissue repair and the effectiveness of immunotherapy. In contrast to "passive response" strategies that exploit these signals merely as triggers for drug release, 3D-printing technology is pioneering a class of "active regulation" paradigms: through the use of functionalized scaffolds designed to alleviate hypoxia, scavenge excess ROS, or neutralize acidic conditions, this approach fundamentally re-engineers the TME to create a milieu more conducive to tumor clearance and tissue regeneration.

Alleviating tumor hypoxia is a critical prerequisite for overcoming immunosuppression and enhancing therapeutic sensitivity. The hypoxic TME, stemming from aberrant vascularization and rapid tumor cell proliferation, not only promotes tumor cell invasion and therapy resistance but also drives the recruitment of immunosuppressive cells via HIF-1α upregulation, thereby severely limiting the efficacy of postoperative multimodal therapy. To address this challenge, Xu *et al.*[90] fabricated a composite oxygen-releasing scaffold comprising polycaprolactone (PCL), nano-hydroxyapatite (n-HA), magnesium peroxide (MgO_2), and polydopamine (PDA) by uniformly incorporating MgO_2 powder into the scaffold matrix via 3D-printing. *In vitro* and *in vivo* subcutaneous tumor models demonstrated that the scaffold's local oxygen-releasing capability not only induced potent pro-apoptotic effects in osteosarcoma cells and suppressed their proliferation but also downregulated heat shock protein 60 (HSP60) expression, thereby significantly potentiating the photothermal therapeutic effect of PDA. Loading bioactive enzymes onto 3D-printed scaffolds represents another potent strategy for modulating the tumor microenvironment. A notable implementation of this approach is the work by Liu *et al.*,[91] who engineered a 3D-printed, sustained-release microneedle patch (MNs@GFD) integrated with GAFe@DOX (GFD) nanozymes. This platform facilitates localized oxygen generation through its robust catalase- and peroxidase-like activities, effectively alleviating intratumoral hypoxia. By bypassing the blood-brain barrier and providing site-specific drug delivery, this enzyme-functionalized system not only remolds the biochemical landscape but also sensitizes glioma cells to chemotherapy by triggering ferroptosis-mediated mitochondrial collapse.

The localized acidic microenvironment and lactic acid accumulation in tumors are key drivers of tumor immune suppression. In the previously described gut microbiota-based, piezoelectric nanobio hybrid microrobot (EA@BTO) system developed by Kang *et al.*,[64] a redox reaction occurs on the surface of the $BaTiO_3$ nanoparticles under the combined influence of the acidic TME and ultrasound stimulation, leading to lactic acid consumption and alleviation of the acidic environment. Following partial neutralization of the acidic microenvironment, the researchers observed enhanced dendritic cell maturation, macrophage polarization toward the M1 phenotype, and a decreased proportion of regulatory T cells, indicating an indirect enhancement of anti-tumor immunity.

Scavenging excess ROS to restore redox homeostasis establishes a pro-regenerative microenvironment conducive to tissue repair. Postoperative wounds and bone defects are often accompanied by inflammatory responses, and excessive ROS accumulation not only inflicts direct damage on surrounding healthy cells but also impairs osteogenic differentiation through the activation of pro-inflammatory signaling pathways[92]. Chen *et al.*[93] immobilized manganese dioxide (MnO_2) nanoparticles onto 3D-printed α-tricalcium phosphate (α-TCP) scaffolds, thereby conferring ROS-scavenging capabilities upon the scaffolds via the enzyme-mimetic activity of MnO_2.

5. Clinical translation pathways and challenges

Despite the substantial theoretical potential of 3D-printing technology in modulating the TME, its clinical translation from bench to bedside remains in its infancy. In contrast to the traditional, large-scale pharmaceutical industry, the current clinical translation of 3D-printed drugs and medical devices remains centered on a decentralized, point-of-care manufacturing model. Although several 3D-printed drug products are advancing through clinical trials and regulatory approval pathways, they continue to face multifaceted challenges, including regulatory oversight, production standardization, biocompatibility validation, and clinical adoption.

Point-of-care manufacturing, as a core paradigm for the clinical translation of 3D-printed pharmaceuticals, is currently undergoing feasibility validation through ongoing clinical trials. In 2015, the U.S. Food and Drug Administration (FDA) approved the first 3D-printed drug, Spritam® (levetiracetam), which utilizes ZipDose® technology—developed by Aprecia Pharmaceuticals—to address medication adherence challenges associated with swallowing difficulties in epilepsy patients[94]. Although Spritam® is not an oncology drug, its approval marked the first regulatory validation of a 3D-printed pharmaceutical, demonstrating that non-conventional manufacturing processes can satisfy the stringent quality control standards required for pharmaceutical products. This landmark approval has paved the way for the regulatory pathway of personalized cancer therapies. In the field of oncology, Denis *et al.*[95] established a hospital-based 3D-printing platform for a clinical trial, designated OPERA, designed to produce a compounded formulation containing tamoxifen (20 mg) and an antidepressant. The objective was to assess the efficacy of this personalized medication regimen in improving hormone therapy adherence among breast cancer patients. This study was conducted at the Clinical Pharmacy Department of Gustave Roussy Cancer Hospital in France, achieving a key milestone by meeting the high production rate demands of clinical trials while ensuring quality control and one-year storage stability of the compounded formulation. This study systematically demonstrates the complete process of producing complex compounded formulations for clinical trials using 3D-printing technology, in compliance with French regulations for pharmacy compounding. Gómez *et al.* further demonstrated the cost and time advantages of point-of-care manufacturing in oral and maxillofacial tumor surgery, showing that in-hospital 3D-printing can reduce the delivery time of surgical guides and personalized implants from two weeks to 72 hours, compared to outsourcing to the biomedical industry[96]. Preliminary clinical evidence has been gathered for personalized implants in the field of reconstructive surgery following bone tumor resection. Yon *et al.*[97] reported a case series on the application of 3D-printed personalized prostheses in reconstruction following ankle bone tumor resection. The researchers fabricated patient-specific prostheses and osteotomy guides using electron beam melting (EBM) technology with a titanium-aluminum-vanadium (TiAlV) alloy, based on preoperative computed tomography (CT) and magnetic resonance imaging (MRI) data. Follow-up data from three patients demonstrated significant improvements in American Orthopaedic Foot & Ankle Society (AOFAS) scores, and imaging assessments confirmed stable implant positioning and early signs of osseointegration.

Despite the early promise of the aforementioned clinical explorations, the clinical translation of 3D-printed products in oncology still faces multiple systemic hurdles. Central to these is the absence of a dedicated regulatory framework. Gómez *et al*. have detailed the impact of the European Medical Device Regulation (MDR) on in-hospital 3D-printing, highlighting that the new regulation imposes stricter requirements for the classification and certification of personalized medical devices, necessitating that hospitals establish quality management systems compliant with the regulation[96]. The FDA has issued guidance on technical considerations for additively manufactured medical devices, and the EU Medical Device Regulation (MDR 2017/745) has established stricter requirements for medical devices. However, dedicated regulatory pathways for high-risk applications, such as 3D-printed drugs and tumor immunotherapies, have yet to be established. Furthermore, the lack of standardized sterilization protocols remains a technical bottleneck. While a study by Babaei *et al.*[98] preliminarily verified the safety of gamma irradiation on PCL/HA scaffolds, it also noted that irradiation can alter material properties, such as reducing hydrophobicity and water uptake capacity, underscoring the need for

Table 3. Summary of 3D-printed systems for modulating key components of the tumor microenvironment

TME-related barriers	Controlled release	3D printing technology	3D printing materials	Regulate strategy	Ref.
Immune microenvironment		Extrusion-based 3D printing	CPC; HAMA	By loading and sustained-release of CSF-1R inhibitors onto the hydrogel layer, the CSF-1R/NF-κB pathway is blocked, thereby inhibiting the polarization of M2-type macrophages and the differentiation of osteoclasts.	[74]
Immune microenvironment		Extrusion-based 3D printing	CPC; HAMA; OHAMA	The combined delivery system simultaneously blocks the CSF-1R and CD47/SIRPα dual pathways, inhibits the polarization of M2-type macrophages, and enhances their ability to engulf tumor cells.	[75]
Immune microenvironment	Near-infrared response	Extrusion-based light-curing 3D printing	GelMA; CQDs; LAP	The CQD in the scaffold can release anti-tumor drugs upon near-infrared stimulation, and it can also induce the polarization of macrophages to the M2 phenotype through immune interactions with macrophages.	[79]
Immune microenvironment	Microstructural design	DLP chip-based projection micro-stereolithography 3D-printing	High-Temperature Light-curable resin; PDMS; HA	Utilizing the self-locking micro-needle structure to achieve precise puncture and anchoring, the anti-PD-L1 antibody and SD-208 combination drug are delivered percutaneously to the local area of melanoma, enhancing the T-cell-mediated anti-tumor immune response.	[52]
Immune microenvironment		DLP-based 3D printing	PEG-PLGA	Nanopreparations of GSK3 inhibitors are prepared using 3D-printed microfluidic devices, which inhibit the expression of PD-1 on CAR-T cells, and enhance the survival, proliferation and memory phenotype of T cells.	[80]
Immune microenvironment	Core-shell structure design	Coaxial 3D printing	PLGA; gelatin; sodium alginate	The outer layer releases the STING agonist to activate the immune pathway, while the core releases the AKT inhibitor to block the negative feedback loop. Together, they enhance the activation of STING and promote the maturation of DCs, the polarization of M1 cells, and the killing of T cells.	[81]
Immune microenvironment	ROS response	Extrusion-based 3D printing	PVA; TSPBA	ROS responds to the hydrogel-loaded ferroptosis inducer RSL3, releasing it and inducing ferroptosis when the tumor recurs. At the same time, it increases CD4+/CD8+ T cells and M1 macrophages, and reduces M2 macrophages.	[59]
Immune microenvironment	Multi-layer structure design	Extrusion-based 3D printing	PLGA; sodium alginate; gelatin	The interlayer dual-drug depot achieves sequential release: MSA-2 is released first to induce immunogenic apoptosis and activate the STING pathway, and DOX is released subsequently to enhance the immune response, jointly initiating a long-lasting cascade immune response.	[83]

(*Cont'd...*)

Table 3. (*Continued*)

TME-related barriers	Controlled release	3D printing technology	3D printing materials	Regulate strategy	Ref.
Immune microenvironment		Stereolithography 3D printing	BioMed clear resin	The dual-storage platform continuously releases immune adjuvants and tumor antigens, locally recruits dendritic cells, and promotes their antigen exposure and activation.	[84]
Immune microenvironment		Extrusion-based 3D printing	GelMA	3D porous scaffolds encapsulate DC and overexpressed PD-1 tumor vesicles, enhancing the activity of DC and the rate of lymph node homing. At the same time, PD1-CVs stimulate DC maturation and block PD-L1, synergistically enhancing DC-mediated anti-tumor immunity.	[86]
Immune microenvironment		Extrusion-based 3D printing	GelMA	The 3D scaffold was used to encapsulate BM-MNCs, tumor lysates and stimulating factors in situ, thereby inducing the differentiation of BM-MNCs into DCs and promoting their maturation and lymph node homing.	[87]
Abnormal vasculature		Extrusion-based 3D printing	PLGA; PVA; sodium alginate; gelatin	The porous scaffold rapidly absorbs blood and disperses tumor cells. CA4 releases to destroy blood vessels first, cutting off the tumor's nutrient supply. DOX is used for slow-release to kill residual cells in the periphery.	[88]
Abnormal vasculature	Multi-region design; magnetic response; enzyme response	Two-photon polymerization 3D-printing	GelMA, LAP, PEG	Multimodal drug-loaded micro-robots actively target tumors. The head and body are respectively loaded with ASA and DOX. They are triggered to release by proteases, and work together to damage blood vessels and kill tumor cells.	[47]
Abnormal vasculature		Extrusion-based 3D printing	Medical grade collagen ink	Encapsulating anti-angiogenic factors and loading them onto 3D-printed scaffolds enables spatial-specific distribution and local sustained release, targeting pathological blood vessels.	[89]
Hypoxia		Extrusion-based 3D printing	PCL; nano-hydroxyapatite; nano MgO2	The continuous oxygen release from MgO_2 in the scaffold improves tumor hypoxia. Meanwhile, the long-term oxygen release in combination with PCL/nHA synergistically promotes osteogenic differentiation, achieving the integration of tumor clearance and bone repair after osteosarcoma surgery.	[90]
Hypoxia	pH response	Projection-based stereolithography bioprinting	GelMA; HAMA; LAP	GAFe@DOX dissociates in acidic microenvironment, DOX induces apoptosis, and the combination of GA and Fe^{3+} catalyzes the Fenton reaction continuously to produce ROS, thereby alleviating hypoxia resistance.	[91]

(*Cont'd...*)

Table 3. (*Continued*)

TME-related barriers	Controlled release	3D printing technology	3D printing materials	Regulate strategy	Ref.
Low pH	Core-shell structure design; ultrasonic response	Light-curing 3D printing	GelMA; LAP	The surface of $BaTiO_3$ nanoparticles undergoes redox reactions under the acidic TME and ultrasonic stimulation. Lactic acid is depleted, thereby mitigating the acidic environment.	[64]
Oxidative stress		Extrusion-based 3D printing	α-TCP; MnO2; SA	By loading MnO_2 to remove local excessive ROS, the oxidative stress in the microenvironment is attenuated, the proliferation and osteogenic differentiation of BMSCs are enhanced, and bone defect repair is promoted.	[93]

Abbreviations: AKT: Protein kinase B; ASA: Acetylsalicylic acid; $BaTiO_3$: Barium titanate; BM-MNCs: Bone marrow mononuclear cells; BMSCs: Bone marrow mesenchymal stem cells; CA4: Combretastatin A4; CAR-T: Chimeric antigen receptor T cell; CD: Cluster of differentiation; CPC: Calcium phosphate ceramic; CQDs: Carbon quantum dots; CSF-1R: Colony-stimulating factor 1 receptor; DCs: Dendritic cells; DLP: Digital light processing; DOX: Doxorubicin; ECM: Extracellular matrix; GAFe@DOX: Gambogic acid–iron nanozyme loaded with doxorubicin; GelMA: Gelatin methacryloyl; GSK3: Glycogen synthase kinase 3; HA: Hyaluronic acid/sodium hyaluronate; HAMA: Methacrylated hyaluronic acid; LAP: Lithium phenyl-2,4,6-trimethylbenzoylphosphinate; MDR: Multidrug resistance; MSA-2: A non-nucleotide STING agonist; NF-κB: Nuclear factor kappa B; nHA: Nano-hydroxyapatite; NIR: Near-infrared; OHAMA: Oxidized methacrylated hyaluronic acid; PD-1: Programmed cell death protein 1; PD-L1: Programmed death-ligand 1; PDMS: Polydimethylsiloxane; PEG: Poly(ethylene glycol); PEG-PLGA: Poly(ethylene glycol)-poly(lactide-co-glycolide); PCL: Polycaprolactone; PLGA: Poly(lactic-co-glycolic acid); PVA: Poly(vinyl alcohol); ROS: Reactive oxygen species; RSL3: Ras-selective lethal 3; SA: Sodium alginate; SD-208: Transforming growth factor-β receptor I kinase inhibitor; SIRPα: Signal regulatory protein α; STING: Stimulator of interferon genes; TME: Tumor microenvironment; TSPBA: ROS-sensitive boronic-acid-based crosslinker; α-TCP: α-Tricalcium phosphate.

material-specific validation of sterilization effects. In addition, production scalability remains a critical issue, as the large number of dosing units required for oncological clinical trials poses significant challenges to batch-to-batch consistency within point-of-care manufacturing models. Batch-to-batch consistency is particularly critical for cell-laden 3D-bioprinted systems, as manufacturing reproducibility is determined not only by printing parameters but also by the intrinsic variability of bioinks. This issue is especially pertinent for naturally derived hydrogels, including gelatin, alginate, collagen, fibrin and hyaluronic acid. Variations in bioink properties, such as source, methacrylation degree and molecular weight, may affect rheological behavior, gelation, mechanical stability, and ultimately the reproducibility of printed drug delivery systems[99]. GelMA and sodium alginate serve as representative examples: the former is sensitive to the source of gelatin and the degree of methacrylation, while the latter is strongly influenced by molecular weight and the composition of mannuronic and guluronic acids[100,101]. Therefore, future translational studies should define material-specific quality attributes and acceptance criteria, including standardized raw material sourcing, chemical and rheological characterization, gelation/degradation testing, lot-release assessment of mechanical properties and drug release profiles, and biological potency assays for cell-laden constructs.

These examples indicate that point-of-care 3D-printing diverges from conventional pharmaceutical manufacturing in several critical aspects, including production location, validation logic, sterility assurance, quality control, and product release procedures. A summary of these key differences is presented in Table 4. In summary, the clinical translation of 3D-printing technology in oncology has established a clear trajectory for point-of-care manufacturing of personalized therapeutics. However, the absence of a dedicated regulatory framework, outdated quality standards, inconsistencies in sterilization protocols, and scalability challenges remain major barriers that impede widespread clinical adoption. Future efforts to advance clinical translation should focus on three core priorities: First, the regulatory framework must be specialized, establishing clear quality standards and approval guidelines that address the unique attributes of 3D-printed oncological products—such as controlled drug spatial distribution, interlayer architecture, and patient-specific geometries—thereby addressing the current regulatory gaps left by the U.S. Food and Drug Administration FDA and European Medicines Agency (EMA). Second, the production paradigm must evolve from bespoke laboratory fabrication to standardized, hospital-level manufacturing. This requires establishing robust links between patient data, printing parameters, and final product quality to ensure batch-to-batch consistency

Table 4. Key operational differences between point-of-care 3D printing and conventional pharmaceutical manufacturing

	Point-of-care 3D printing	Conventional pharmaceutical manufacturing
Manufacturing model	Decentralized or hospital-based production, often tailored to individual patients, local anatomy, or treatment regimens	Centralized large-scale production using fixed formulations, standardized equipment, and validated batch or continuous manufacturing processes
Product variability	Intended variability may be part of the design, including patient-specific geometry, dose, drug combination, or release profile	Variability is minimized; products are manufactured to predefined specifications with limited allowable batch-to-batch variation
Validation	Requires validation of the printer, material, software workflow, printing parameters, post-processing, and operator-dependent steps; validation may need to account for design-specific changes	Relies on established process validation for a fixed product and manufacturing process, with defined critical process parameters and critical quality attributes
Sterility and contamination control	Sterility assurance is challenging because production, post-processing, packaging, and sterilization may occur in or near clinical environments	Sterility control is performed within dedicated facilities using validated cleanroom, aseptic processing, terminal sterilization, and environmental monitoring systems
Lot release	Release decisions may need to be made at the level of an individual patient-specific unit or small production run, requiring clear responsibility between hospital, manufacturer, and regulatory body	Lot release is performed for defined batches according to established specifications, quality documentation, and regulatory requirements
Scalability	Suited for personalized or small-batch production but challenged by throughput, staff training, quality consistency, and reproducibility across sites	Suited for high-throughput production with mature supply chains, validated equipment, and standardized quality systems

and traceability within the point-of-care model. Finally, clinical validation must transition from anecdotal case reports to prospective, well-controlled clinical trials. Rigorously designed studies across diverse tumor subtypes are essential to generate robust long-term safety and efficacy data, ultimately advancing this technology from preclinical promise to established clinical practice.

6. Conclusion

This review highlights the promise of 3D printing and bioprinting as enabling technologies for spatiotemporally controlled drug delivery within the TME. By integrating acellular and cell-laden systems, these platforms allow drug distribution and release to be engineered through spatial compartmentalization, gradient architectures, microstructural design, programmable degradation, and biologically active components, thereby offering new strategies to address key TME barriers, including aberrant vasculature, dense extracellular matrix, immune heterogeneity, and metabolic dysregulation. Importantly, their value lies not only in improving local drug retention and release kinetics, but also in enabling delivery systems to participate in partial TME remodeling and functional reprogramming. Nevertheless, current platforms remain constrained by material biocompatibility, printing resolution, biological stability, manufacturing scalability, and clinical translation. Future progress should therefore focus on three priorities: spatially informed, patient-specific design that integrates tumor imaging, spatial omics, and AI-assisted inverse design to guide construct geometry and regional drug loading; adaptive delivery systems that couple local TME sensing with feedback-regulated or externally triggered release; and regulatory-grade manufacturing standards for 3D-printed oncological combination products, including spatial dose accuracy, interlayer reproducibility, sterilization compatibility, degradation behavior, biosafety, and batch-to-batch consistency. Advancing along these directions will be important for transforming 3D/bioprinting-based delivery systems from customizable experimental constructs into reproducible, adaptive, and clinically actionable cancer therapies.

Acknowledgments

None.

Funding

This work was supported by research development fund for talent startup project of Jiyang College, Zhejiang A&F University (RC2025F02), General Scientific Research Project of Zhejiang Provincial Department of Education in 2025 (Y202558493), and the special research fund of the China Pearl College (JYZZ202506).

Conflict of interest

The authors declare that they have no conflict of interest related to this work.

Author contributions

Conceptualization: Yuan Wu, Zhouyi Sun, Zihao Guo
Supervision: Zihao Guo, Zhouyi Sun
Visualization: Yaying Xu, Jukai Zhang, Yile Wang
Writing–original draft: Yuan Wu
Writing–review & editing: Yuan Wu, Zhouyi Sun, Zihao Guo

All authors approved the final version.

Ethics approval and consent to participate

Not applicable.

Consent for publication

Not applicable.

Availability of data

Not applicable.

References

1. He Q, Chen J, Yan J, *et al*. Tumor microenvironment responsive drug delivery systems. *Asian J Pharm Sci*. 2020;15(4):416-448.

   doi: 10.1016/j.ajps.2019.08.003

2. Loyher PL, Hamon P, Laviron M, *et al*. Macrophages of distinct origins contribute to tumor development in the lung. *J Exp Med*. 2018;215(10):2536-2553.

   doi: 10.1084/jem.20180534

3. Mo CK, Liu J, Chen S, *et al*. Tumour evolution and microenvironment interactions in 2D and 3D space. *Nature*. 2024;634(8036):1178-1186.

   doi: 10.1038/s41586-024-08087-4

4. Chen Z, Han F, Du Y, Shi H, Zhou W. Hypoxic microenvironment in cancer: molecular mechanisms and therapeutic interventions. *Signal Transduct Target Ther*. 2023;8(1):70.

   doi: 10.1038/s41392-023-01332-8

5. Mitchell MJ, Billingsley MM, Haley RM, Wechsler ME, Peppas NA, Langer R. Engineering precision nanoparticles for drug delivery. *Nat Rev Drug Discov*. 2021;20(2):101-124.

   doi: 10.1038/s41573-020-0090-8

6. Dewhirst MW, Secomb TW. Transport of drugs from blood vessels to tumour tissue. *Nat Rev Cancer*. 2017;17(12):738-750.

   doi: 10.1038/nrc.2017.93

7. Shabbir F, Mujeeb AA, Jawed SF, Khan AH, Shakeel CS. Simulation of transvascular transport of nanoparticles in tumor microenvironments for drug delivery applications. *Sci Rep*. 2024;14(1):1764.

   doi: 10.1038/s41598-024-52292-0

8. Nguyen LNM, Ngo W, Lin ZP, *et al*. The mechanisms of nanoparticle delivery to solid tumours. *Nat Rev Bioeng*. 2024;2(3):201-213.

   doi: 10.1038/s44222-024-00154-9

9. Li J, Mooney DJ. Designing hydrogels for controlled drug delivery. *Nat Rev Mater*. 2016;1(12).

   doi: 10.1038/natrevmats.2016.71

10. Liang S, Wang T, Ding J, Yang J, He C, Rong Y. Injectable Matrix Metalloproteinase-Responsive Polypeptide Hydrogels as Drug Depots for Antitumor Chemo-Immunotherapy. *Pharmaceutics*. 2025;17(11):1453.

    doi: 10.3390/pharmaceutics17111453

11. Kang T, Cha GD, Park OK, *et al*. Penetrative and Sustained Drug Delivery Using Injectable Hydrogel Nanocomposites for Postsurgical Brain Tumor Treatment. *ACS Nano*. 2023;17(6):5435-5447.

    doi: 10.1021/acsnano.2c10094

12. Munoz NM, Williams M, Dixon K, *et al*. Influence of injection technique, drug formulation and tumor microenvironment on intratumoral immunotherapy delivery and efficacy. *J Immunother Cancer*. 2021;9(2):e001800.

    doi: 10.1136/jitc-2020-001800

13. Huang A, Pressnall MM, Lu R, *et al*. Human intratumoral therapy: Linking drug properties and tumor transport of drugs in clinical trials. *J Control Release*. 2020;326:203-221.

    doi: 10.1016/j.jconrel.2020.06.029

14. Datta P, Dey M, Ataie Z, Unutmaz D, Ozbolat IT. 3D bioprinting for reconstituting the cancer microenvironment. *NPJ Precis Oncol*. 2020;4(1):18.

    doi: 10.1038/s41698-020-0121-2

15. Lau K, Tran HA, Tan R, *et al*. Advancements in 3D-printing strategies towards developing effective implantable drug delivery systems: Recent applications and opportunities. *Adv Drug Deliv Rev*. 2025;227:115711.

doi: 10.1016/j.addr.2025.115711

16. Michael B, Jayaprakash N, Munivel N, Jaisankar D. 3D printing in drug delivery: emerging technologies, clinical translation, and the future of personalized medicine. *Med Drug Discov*. 2025:100242.

    doi: 10.1016/j.medidd.2025.100242

17. Yuan T, Fu X, Hu R, *et al*. Bioprinted, spatially defined breast tumor microenvironment models of intratumoral heterogeneity and drug resistance. *Trends Biotechnol*. 2024;42(11):1523-1550.

    doi: 10.1016/j.tibtech.2024.06.007

18. Rodriguez-Gonzalez R, Delgado JA, Delgado LM, Perez RA. Silica 3D printed scaffolds as pH stimuli-responsive drug release platform. *Mater Today Bio*. 2024;28:101187.

    doi: 10.1016/j.mtbio.2024.101187

19. Debnath S, Latiyan S, Jain N, *et al*. 3D Bioprinted Immunomodulation horizontal line The Advancing Landscape of Next-Generation Immuno-oncology. *Biomacromolecules*. 2025;26(6):3255-3280.

    doi: 10.1021/acs.biomac.4c01816

20. Chlenski A, Guerrero LJ, Peddinti R, *et al*. Anti-angiogenic SPARC peptides inhibit progression of neuroblastoma tumors. *Mol Cancer*. 2010;9:138.

    doi: 10.1186/1476-4598-9-138

21. Manzari MT, Shamay Y, Kiguchi H, Rosen N, Scaltriti M, Heller DA. Targeted drug delivery strategies for precision medicines. *Nat Rev Mater*. 2021;6(4):351-370.

    doi: 10.1038/s41578-020-00269-6

22. Goos J, Cho A, Carter LM, *et al*. Delivery of polymeric nanostars for molecular imaging and endoradiotherapy through the enhanced permeability and retention (EPR) effect. *Theranostics*. 2020;10(2):567-584.

    doi: 10.7150/thno.36777

23. Price LSL, Stern ST, Deal AM, Kabanov AV, Zamboni WC. A reanalysis of nanoparticle tumor delivery using classical pharmacokinetic metrics. *Sci Adv*. 2020;6(29):eaay9249.

    doi: 10.1126/sciadv.aay9249

24. Kim YM, Kim H, Park SC, Lee M, Jang MK. Targeted drug delivery of cancer cell-derived extracellular vesicles decorated with a VEGFR-binding peptide. *Colloids Surf B Biointerfaces*. 2025;252:114661.

    doi: 10.1016/j.colsurfb.2025.114661

25. Yuan Z, Li Y, Zhang S, *et al*. Extracellular matrix remodeling in tumor progression and immune escape: from mechanisms to treatments. *Mol Cancer*. 2023;22(1):48.

    doi: 10.1186/s12943-023-01744-8

26. Stylianopoulos T, Jain RK. Combining two strategies to improve perfusion and drug delivery in solid tumors. *Proc Natl Acad Sci U S A*. 2013;110(46):18632-7.

    doi: 10.1073/pnas.1318415110

27. Parodi A, Haddix SG, Taghipour N, *et al*. Bromelain surface modification increases the diffusion of silica nanoparticles in the tumor extracellular matrix. *ACS Nano*. 2014;8(10):9874-9883.

    doi: 10.1021/nn502807n

28. Hu Q, Zhu Y, Mei J, Liu Y, Zhou G. Extracellular matrix dynamics in tumor immunoregulation: from tumor microenvironment to immunotherapy. *J Hematol Oncol*. 2025;18(1):65.

    doi: 10.1186/s13045-025-01717-y

29. Chu X, Tian Y, Lv C. Decoding the spatiotemporal heterogeneity of tumor-associated macrophages. *Mol Cancer*. 2024;23(1):150.

    doi: 10.1186/s12943-024-02064-1

30. He S, Zheng L, Qi C. Myeloid-derived suppressor cells (MDSCs) in the tumor microenvironment and their targeting in cancer therapy. *Mol Cancer*. 2025;24(1):5.

    doi: 10.1186/s12943-024-02208-3

31. Zhou Z, Xu J, Liu S, *et al*. Infiltrating treg reprogramming in the tumor immune microenvironment and its optimization for immunotherapy. *Biomark Res*. 2024;12(1):97.

    doi: 10.1186/s40364-024-00630-9

32. Miller MA, Zheng YR, Gadde S, *et al*. Tumour-associated macrophages act as a slow-release reservoir of nano-therapeutic Pt(IV) pro-drug. *Nat Commun*. 2015;6(1):8692.

    doi: 10.1038/ncomms9692

33. Lin ZP, Nguyen LNM, Ouyang B, *et al*. Macrophages Actively Transport Nanoparticles in Tumors After Extravasation. *ACS Nano*. 2022;16(4):6080-6092.

    doi: 10.1021/acsnano.1c11578

34. Wang L, Zhang L, Zhang Z, Wu P, Zhang Y, Chen X. Advances in targeting tumor microenvironment for immunotherapy. *Front Immunol*. 2024;15:1472772.

    doi: 10.3389/fimmu.2024.1472772

35. Liao C, Liu X, Zhang C, Zhang Q. Tumor hypoxia: From basic knowledge to therapeutic implications. *Semin Cancer Biol*. 2023;88:172-186.

    doi: 10.1016/j.semcancer.2022.12.011

36. Cognet G, Muir A. Identifying metabolic limitations in the tumor microenvironment. *Sci Adv*. 2024;10(40):eadq7305.

    doi: 10.1126/sciadv.adq7305

37. Bao MHR, Wong CCL. Hypoxia, Metabolic Reprogramming, and Drug Resistance in Liver Cancer. *Cells*. 2021;10(7):1715.

    doi: 10.3390/cells10071715

38. Ahmed Z, LoGiudice K, Mays G, *et al*. Increasing Chemotherapeutic Efficacy Using pH-Modulating and Doxorubicin-Releasing Injectable Chitosan-Poly(ethylene glycol) Hydrogels. *ACS Appl Mater Interfaces*. 2023;15(39):45626-45639.

doi: 10.1021/acsami.3c09733

39. Liu Y, Si L, Jiang Y, *et al*. Design of pH-Responsive Nanomaterials Based on the Tumor Microenvironment. *Int J Nanomedicine*. 2025;20:705-721.

doi: 10.2147/IJN.S504629

40. Jin Z, Al Amili M, Guo S. Tumor Microenvironment-Responsive Drug Delivery Based on Polymeric Micelles for Precision Cancer Therapy: Strategies and Prospects. *Biomedicines*. 2024;12(2):417.

doi: 10.3390/biomedicines12020417

41. Xu X, Zhao J, Wang M, Wang L, Yang J. 3D Printed Polyvinyl Alcohol Tablets with Multiple Release Profiles. *Sci Rep*. 2019;9(1):12487.

doi: 10.1038/s41598-019-48921-8

42. Li J, Wu M, Chen W, *et al*. 3D printing of bioinspired compartmentalized capsular structure for controlled drug release. *J Zhejiang Univ Sci B*. 2021;22(12):1022-1033.

doi: 10.1631/jzus.B2100644

43. Kyobula M, Adedeji A, Alexander MR, *et al*. 3D inkjet printing of tablets exploiting bespoke complex geometries for controlled and tuneable drug release. *J Control Release*. 2017;261:207-215.

doi: 10.1016/j.jconrel.2017.06.025

44. Myung N, Jin S, Cho HJ, Kang HW. User-designed device with programmable release profile for localized treatment. *J Control Release*. 2022;352:685-699.

doi: 10.1016/j.jconrel.2022.10.054

45. Myung N, Kang HW. Local dose-dense chemotherapy for triple-negative breast cancer via minimally invasive implantation of 3D printed devices. *Asian J Pharm Sci*. 2024;19(1):100884.

doi: 10.1016/j.ajps.2024.100884

46. Hagan CT, Bloomquist C, Kim I, *et al*. Continuous liquid interface production of 3D printed drug-loaded spacers to improve prostate cancer brachytherapy treatment. *Acta Biomater*. 2022;148:163-170.

doi: 10.1016/j.actbio.2022.06.023

47. Li Y, Dong D, Qu Y, *et al*. A Multidrug Delivery Microrobot for the Synergistic Treatment of Cancer. *Small*. 2023;19(44):e2301889.

doi: 10.1002/smll.202301889

48. Fang Y, Luo X, Xu Y, *et al*. Sandwich-Structured Implants to Obstruct Multipath Energy Supply and Trigger Self-Enhanced Hypoxia-Initiated Chemotherapy Against Postsurgical Tumor Recurrence and Metastasis. *Adv Sci (Weinh)*. 2023;10(22):e2300899.

doi: 10.1002/advs.202300899

49. Zhou L, Zhao S, Xu Y, *et al*. Spatial-Constraint Modulation of Intra/Extracellular Reactive Oxygen Species by Adaptive Hybrid Materials for Boosting Pyroptosis and Combined Immunotherapy of Breast Tumor. *Adv Healthc Mater*. 2025;14(17):e2500371.

doi: 10.1002/adhm.202500371

50. Yi HG, Choi YJ, Kang KS, *et al*. A 3D-printed local drug delivery patch for pancreatic cancer growth suppression. *J Control Release*. 2016;238:231-241.

doi: 10.1016/j.jconrel.2016.06.015

51. Hagan IV CT, Bloomquist C, Warner S, *et al*. 3D printed drug-loaded implantable devices for intraoperative treatment of cancer. *J Control Release*. 2022;344:147-156.

doi: 10.1016/j.jconrel.2022.02.024

52. Joo SH, Kim J, Hong J, Fakhraei Lahiji S, Kim YH. Dissolvable Self-Locking Microneedle Patches Integrated with Immunomodulators for Cancer Immunotherapy. *Adv Mater*. 2023;35(10):e2209966.

doi: 10.1002/adma.202209966

53. Tamjid E, Bohlouli M, Mohammadi S, Alipour H, Nikkhah M. Sustainable drug release from highly porous and architecturally engineered composite scaffolds prepared by 3D printing. *J Biomed Mater Res A*. 2020;108(6):1426-1438.

doi: 10.1002/jbm.a.36914

54. Sultan S, Mathew AP. 3D printed scaffolds with gradient porosity based on a cellulose nanocrystal hydrogel. *Nanoscale*. 2018;10(9):4421-4431.

doi: 10.1039/c7nr08966j

55. Wu X, Chen K, Chai Q, *et al*. A 3D printed multilayer biomimetic scaffold with a gradient-oriented structure for articular cartilage repair. *J Mater Chem B*. 2025;13(26):7728-7743.

doi: 10.1039/d5tb00383k

56. Fan D, Zhang C, Wang H, *et al*. Fabrication of a composite 3D-printed titanium alloy combined with controlled in situ drug release to prevent osteosarcoma recurrence. *Mater Today Bio*. 2023;20:100683.

doi: 10.1016/j.mtbio.2023.100683

57. Zaer M, Moeinzadeh A, Abolhassani H, *et al*. Doxorubicin-loaded Niosomes functionalized with gelatine and alginate as pH-responsive drug delivery system: A 3D printing approach. *Int J Biol Macromol*. 2023;253(Pt 2):126808.

doi: 10.1016/j.ijbiomac.2023.126808

58. Kefayat A, Molaabasi F, Bahrami M, *et al*. 3D printed,

biodegradable, and biocompatible intraperitoneal implants loaded with folic acid-targeted/pH-sensitive/doxorubicin-loaded hydroxyapatite nanoparticles for systemic treatment of metastatic breast cancer. *J Nanobiotechnology*. 2025;24(1):39.

doi: 10.1186/s12951-025-03854-5

59. Wang L, Ye C, Xue X, *et al*. 3D-Printed Breast Prosthesis that Smartly Senses and Targets Breast Cancer Relapse. *Adv Sci (Weinh)*. 2024;11(46):e2402345.

doi: 10.1002/advs.202402345

60. Su Q, Wang Z, Li P, Wei X, Xiao J, Duan X. pH and ROS Dual-Responsive Autocatalytic Release System Potentiates Immunotherapy of Colorectal Cancer. *Adv Healthc Mater*. 2024;13(29):e2401126.

doi: 10.1002/adhm.202401126

61. Zhang X, Lian R, Fan B, *et al*. ROS/Enzyme Dual-Responsive Drug Delivery System for Targeted Colorectal Cancer Therapy: Synergistic Chemotherapy, Anti-Inflammatory, and Gut Microbiota Modulation. *Pharmaceutics*. 2025;17(7):940.

doi: 10.3390/pharmaceutics17070940

62. Hadipour Moghaddam SP, Yazdimamaghani M, Ghandehari H. Glutathione-sensitive hollow mesoporous silica nanoparticles for controlled drug delivery. *J Control Release*. 2018;282:62-75.

doi: 10.1016/j.jconrel.2018.04.032

63. Shen J, Wang Q, Fang J, *et al*. Therapeutic polymeric nanomedicine: GSH-responsive release promotes drug release for cancer synergistic chemotherapy. *RSC Adv*. 2019;9(64):37232-37240.

doi: 10.1039/c9ra07051f

64. Kang Y, She Y, Zang Y, *et al*. Biohybrid Microrobot Enteric-Coated Microcapsule for Oral Treatment of Colorectal Cancer. *Adv Mater*. 2025;37(40):e20586.

doi: 10.1002/adma.202420586

65. Yang C, Zhao W, Zhang L, *et al*. Intradermal Delivery of Cell Vaccine via Ice Microneedles for Cancer Treatment. *Adv Healthc Mater*. 2025;14(1):e2400678.

doi: 10.1002/adhm.202400678

66. Kim D, Jo S, Lee D, *et al*. NK cells encapsulated in micro/macropore-forming hydrogels via 3D bioprinting for tumor immunotherapy. *Biomater Res*. 2023;27(1):60.

doi: 10.1186/s40824-023-00403-9

67. Xia P, Liu C, Wei X, Guo J, Luo Y. 3D-Printed hydrogel scaffolds with drug- and stem cell-laden core/shell filaments for cancer therapy and soft tissue repair. *J Mater Chem B*. 2024;12(44):11491-11501.

doi: 10.1039/d4tb01571a

68. Liu H, Shi X, Wang D, Zhang H, Xu Z, Tan Z. Three-Dimensional-Printed In Vitro Model of Colorectal Cancer with Immune Microenvironment and Reprogramming Capabilities. *ACS Biomater Sci Eng*. 2025;11(10):5991-6003.

doi: 10.1021/acsbiomaterials.5c00263

69. Xu HQ, Liu JC, Zhang ZY, Xu CX. A review on cell damage, viability, and functionality during 3D bioprinting. *Mil Med Res*. 2022;9(1):70.

doi: 10.1186/s40779-022-00429-5

70. Elango J, Zamora-Ledezma C. Rheological, Structural, and Biological Trade-Offs in Bioink Design for 3D Bioprinting. *Gels*. 2025;11(8):659

doi: 10.3390/gels11080659

71. Martin KE, Hammer Q, Perica K, Sadelain M, Malmberg KJ. Engineering immune-evasive allogeneic cellular immunotherapies. *Nat Rev Immunol*. 2024;24(9):680-693.

doi: 10.1038/s41577-024-01022-8

72. Sun R, Jiao Y, Chen J, *et al*. Neutrophil-Mediated Delivery Platforms for Synergistic Chemo-Immunotherapy of Non-Small-Cell Lung Cancer Therapy. *Nano Lett*. 2025;25(38):14229-14236.

doi: 10.1021/acs.nanolett.5c04210

73. Zhang Y, Xu J, Fei Z, *et al*. 3D Printing Scaffold Vaccine for Antitumor Immunity. *Adv Mater*. 2021;33(48):e2106768.

doi: 10.1002/adma.202106768

74. Li C, Li C, Ma Z, *et al*. Regulated macrophage immune microenvironment in 3D printed scaffolds for bone tumor postoperative treatment. *Bioact Mater*. 2023;19:474-485.

doi: 10.1016/j.bioactmat.2022.04.028

75. Li C, Ma Z, Sun X, *et al*. Activation of bone tumor-eating macrophages via assembling and co-delivering 3D printed scaffold. *Biomaterials*. 2026;324:123495.

doi: 10.1016/j.biomaterials.2025.123495

76. Qu T, Li B, Wang Y. Targeting CD47/SIRPalpha as a therapeutic strategy, where we are and where we are headed. *Biomark Res*. 2022;10(1):20.

doi: 10.1186/s40364-022-00373-5

77. Huang M, Zhang L, Cui J, *et al*. 3D printing of GelMA/nanohydroxyapatite/melanin nanoparticles composite hydrogel scaffolds for bone regeneration through immunomodulation. *Int J Biol Macromol*. 2025;306(Pt 2):141453.

doi: 10.1016/j.ijbiomac.2025.141453

78. Wang C, Wu Q, Zhuang L, *et al*. Immunometabolism of macrophages in the bone microenvironment: a new perspective for bone healing therapy. *J Adv Res*. 2026;82:485-506.

doi: 10.1016/j.jare.2025.07.046

79. Dutta SD, Ganguly K, Hexiu J, Randhawa A, Moniruzzaman M, Lim KT. A 3D Bioprinted Nanoengineered Hydrogel with Photoactivated Drug Delivery for Tumor Apoptosis and Simultaneous Bone Regeneration via Macrophage Immunomodulation. *Macromol Biosci*. 2023;23(9):e2300096.

doi: 10.1002/mabi.202300096

80. Badiee P, Maritz MF, Thierry B. Glycogen kinase 3 inhibitor nanoformulation as an alternative strategy to inhibit PD-1 immune checkpoint. *Int J Pharm*. 2022;622:121845.

doi: 10.1016/j.ijpharm.2022.121845

81. Wang H, Liu Z, Fang Y, *et al*. Spatiotemporal release of non-nucleotide STING agonist and AKT inhibitor from implantable 3D-printed scaffold for amplified cancer immunotherapy. *Biomaterials*. 2024;311:122645.

doi: 10.1016/j.biomaterials.2024.122645

82. Yin M, Mao L, Zhang X, *et al*. Biodegradable 3D Injectable Amino Acid Hydrogels Delivering Immune Adjuvant for Enhancing Immunotherapy in Colon Cancer. *Cancer Sci*. 2025;116(10):2846-2857.

doi: 10.1111/cas.70156

83. Li K, Yu X, Xu Y, *et al*. Cascaded immunotherapy with implantable dual-drug depots sequentially releasing STING agonists and apoptosis inducers. *Nat Commun*. 2025;16(1):1629.

doi: 10.1038/s41467-025-56407-7

84. Kota N, Gonzalez DD, Liu HC, *et al*. Prophylactic and therapeutic cancer vaccine with continuous localized immunomodulation. *Nanomedicine*. 2024;62:102776.

doi: 10.1016/j.nano.2024.102776

85. Xie D, Han C, Chen C, *et al*. A scaffold vaccine to promote tumor antigen cross-presentation via sustained toll-like receptor-2 (TLR2) activation. *Bioact Mater*. 2024;37:315-330.

doi: 10.1016/j.bioactmat.2024.03.035

86. Xu Y, Zhu W, Wu J, *et al*. 3D-Printed Dendritic Cell Vaccines for Post-Surgery Cancer Immunotherapy. *Adv Funct Mater*. 2024;34(33):2400507.

doi: 10.1002/adfm.202400507

87. Chen L, Xu Y, Hu X, *et al*. In situ generation of dendritic cell vaccines in 3D printing scaffolds for cancer post-surgical therapy. *Natl Sci Rev*. 2026;13(5):nwag037.

doi: 10.1093/nsr/nwag037

88. Fang Y, Liu Z, Wang H, *et al*. Implantable Sandwich-like Scaffold/Fiber Composite Spatiotemporally Releasing Combretastatin A4 and Doxorubicin for Efficient Inhibition of Postoperative Tumor Recurrence. *ACS Appl Mater Interfaces*. 2022;14(24):27525-27537.

doi: 10.1021/acsami.2c02103

89. Abbadessa A, Nunez Bernal P, Buttitta G, *et al*. Biofunctionalization of 3D printed collagen with bevacizumab-loaded microparticles targeting pathological angiogenesis. *J Control Release*. 2023;360:747-758.

doi: 10.1016/j.jconrel.2023.07.017

90. Xu H, Peng Z, Lin J, *et al*. 3D-Printed Magnesium Peroxide-Incorporated Scaffolds with Sustained Oxygen Release and Enhanced Photothermal Performance for Osteosarcoma Multimodal Treatments. *ACS Appl Mater Interfaces*. 2024;16(8):9626-9639.

doi: 10.1021/acsami.3c10807

91. Liu M, Qiao Y, Cheng S, *et al*. 3D bioprinted microneedle patches loaded with gambogic acid-iron-doxorubicin nanozymes for postoperative glioma in situ therapy via ferroptosis synergistic chemosensitization. *J Nanobiotechnology*. 2025;23(1):755.

doi: 10.1186/s12951-025-03790-4

92. Chao Y, Liu Z. Biomaterials tools to modulate the tumour microenvironment in immunotherapy. *Nat Rev Bioeng*. 2023;1(2):125-138.

doi: 10.1038/s44222-022-00004-6

93. Chen P, Xia Y, Wu Y, Wu X, Wang Y, Dai H. 3D-printed scaffolds with ROS-clearing capacity for critical-sized bone defect regeneration. *Biomater Adv*. 2026;180:214575.

doi: 10.1016/j.bioadv.2025.214575

94. First 3D-printed pill. *Nat Biotechnol*. 2015;33(10):1014.

doi: 10.1038/nbt1015-1014a

95. Denis L, Jorgensen AK, Do B, *et al*. Developing an innovative 3D printing platform for production of personalised medicines in a hospital for the OPERA clinical trial. *Int J Pharm*. 2024;661:124306.

doi: 10.1016/j.ijpharm.2024.124306

96. Gómez VJ, Martin-Gonzalez A, Zafra-Vallejo V, Zubillaga-Rodriguez I, Fernandez-Garcia A, Sanchez-Aniceto G. Controversies in point-of-care 3D printing for oncological and reconstructive surgery with free software in oral and maxillofacial surgery: European regulations, costs, and timeframe. *Int J Oral Maxillofac Surg*. 2024;53(8):650-660.

doi: 10.1016/j.ijom.2024.01.005

97. Yon CJ, Choi BC, Lee JM, Lee SW. Personalized 3D-Printed Prostheses for Bone Defect Reconstruction After Tumor Resection in the Foot and Ankle. *J Funct Biomater*. 2025;16(2):62.

doi: 10.3390/jfb16020062

98. Babaei M, Ebrahim-Najafabadi N, Mirzadeh M, *et al*. A comprehensive bench-to-bed look into the application of gamma-sterilized 3D-printed polycaprolactone/hydroxyapatite implants for craniomaxillofacial defects, an in vitro, in vivo, and clinical study. *Biomater Adv*.

2024;161:213900.

doi: 10.1016/j.bioadv.2024.213900

99. Chen XB, Fazel Anvari-Yazdi A, Duan X, *et al*. Biomaterials / bioinks and extrusion bioprinting. *Bioact Mater*. 2023;28:511-536.

doi: 10.1016/j.bioactmat.2023.06.006

100. Gaglio CG, Baruffaldi D, Pirri CF, Napione L, Frascella F. GelMA synthesis and sources comparison for 3D multimaterial bioprinting. *Front Bioeng Biotechnol*. 2024;12:1383010.

doi: 10.3389/fbioe.2024.1383010

101. Jiao W, Chen W, Mei Y, *et al*. Effects of Molecular Weight and Guluronic Acid/Mannuronic Acid Ratio on the Rheological Behavior and Stabilizing Property of Sodium Alginate. *Molecules*. 2019;24(23):4374.

doi: 10.3390/molecules24234374